UNIVERSITY OF OKLAHOMA

GRADUATE COLLEGE

EFFECTS OF PRESSURE AND OIL CONTAMINATION ON DRAINAGE AND BUBBLE SIZE DISTRIBUTION OF AQUEOUS FOAMS

A THESIS

SUBMITTED TO THE GRADUATE FACULTY

in partial fulfillment of the requirements for the

Degree of

MASTER OF SCIENCE

By

KARAN DINESH SHAH

Norman, Oklahoma

2022

EFFECTS OF PRESSURE AND OIL CONTAMINATION ON DRAINAGE AND BUBBLE SIZE DISTRIBUTION OF AQUEOUS FOAMS

A THESIS APPROVED FOR THE

MEWBOURNE SCHOOL OF PETROLEUM AND GEOLOGICAL ENGINEERING

BY THE COMMITTEE CONSISTING OF

Dr. Ahmed Ramadan, Chair

Dr. Catalin Teodoriu

Dr. Hamidreza Karami

ACKNOWLEDGEMENTS

First and foremost, I want to thank God for all his gifts and for leading me along the path to prosperity. I am appreciative of Dr. Ramadan Ahmed for providing me with constant support and immense patience throughout the duration of my thesis. Throughout this journey, I have benefitted from Dr. Ahmed's resources, knowledge, and constructive comments. I have learned the basics of drilling while taking Advanced drilling class with him. He has encouraged me to work hard and helped me develop patience as a researcher. I'm indebted for his inputs that he has provided while technical writing.

Additionally, I would like to express my gratitude to Dr. Catalin Teodoriu and Dr. Hamidreza Karami for taking time out to serve on my thesis committee. My first class at OU with Dr. Catalin was instrumental, both practically as well as theoretically. He has been a great support and very approachable as a Liaison of the department. Dr. Karami has helped me comprehend production engineering in great depth, given that I come from a chemical engineering background.

I'd like to thank Dr. Rida Elgaddafi and Oyindamola for their insights and for explaining the experimental setup and data analysis required for the project. Next, I would like to thank Jeff McCaskill for providing all the technical support required during performing the experiments at WCTC. Thanks to him, I've learned how to use a variety of new tools. I'd like to thank all my fellow researchers at WCTC to help me in different ways.

I'm obliged to my grandfather Ganshi Shah for always encouraging me in my academic endeavors. My heartfelt gratitude to my parents, Dinesh Shah and Bharati Shah, for being my constant rock of support throughout these years. A big thanks to my sister Urvashi Shah for

encouraging me throughout my time away from home. I'd like to thank my cousins and relatives for believing in me and showering their blessings. My friends more like family - Aishwarya, Rashil, Haripriya, Shruti, Jay, and Meet have always been there for me whether it is to celebrate with me or cheer me up when most needed. Lastly, I'm thankful to all the friends I have made at OU for making this journey memorable.

This research was made possible by NPRP grant 10-0115-170165 from the Qatar National Research Fund (QNRF). I would like to thank the Qatar National Research Fund for providing the research fund for this project. Also, I would like to express my gratitude and appreciation to the Texas A&M University at Qatar and the University of Oklahoma for supporting the project.

TABLE OF CONTENTS

LIST OF FIGURES

LIST OF TABLES

ABSTRACT

Foams exhibit valuable properties such as high viscosity, low density, and good cutting carrying capacity. However, they are thermodynamically unstable due to gravitational drainage, bubble coalescence, and coarsening. As a result, they lose these functional properties with time. Therefore, this study investigates the effects of pressure and contaminant oil on the stability of aqueous foams. In a flow loop with a vertical drainage measurement section, nitrogen foam was generated. Drainage experiments were conducted for different (40 - 60%) foam qualities while varying the pressure from 100 to 400 psi. Water with 2% anionic surfactant was used as the base liquid. Tests were also conducted at 10% v/v oil concentration to study the effect of contamination. The foam images were captured using a viewport at regular intervals to examine bubble structure and determine the bubble size distribution with time.

At constant pressure, lower-quality aqueous foams drained faster than higher-quality aqueous foams without oil contamination. On the contrary, when 10% oil was added to the base liquid, 50% quality foam exhibited lower drainage than 40% and 60% quality foams. The stability of aqueous foams also improved considerably when the pressure was increased for each foam quality, regardless of the presence of oil.

The data from image processing showed that as the pressure increases, the bubble size decreases at a constant foam quality. Besides this, bubble size approximately linearly increased with time, demonstrating bubble coalescence and coarsening. Furthermore, the size of the bubbles grew with foam quality. It can be concluded that the increase in pressure stabilizes the aqueous foam. At a given foam quality, the lower the bubble size more stable is the foam. Contaminants like oil affect the aqueous foam's stability and bubble size. This study helps

understand the effect of pressure and oil contaminants on the stability of aqueous foam at different quality.

1. CHAPTER ONE

1.1 **Overview**

Foam is created when a dispersed gas phase is trapped in a continuous liquid phase, resulting in a variety of bubble sizes. They contain large volumes of gas separated by thin liquid films. Mechanical agitation or shearing, as well as the presence of a surfactant to reduce surface tension and stabilize the interface between the two phases, are essential to produce foams. In many industrial applications, foams are efficient and economical. In foam drilling operations, the backpressure, and gas and liquid injection rates are all adjusted parameters to manage the foam quality (volumetric concentration of the gas phase). The liquid phase consists of water and surfactants, whereas the gas phase consists of either air, nitrogen, carbon dioxide, or hydrocarbon gas.

Foams are used in a variety of industries, including food, petroleum, firefighting, pharmaceuticals, personal care goods, sewage treatment, chemical sector, textile, and paper (Kim and Dlugogorski 1996). Common examples of foam products are bath foam, whipped cream, fire retardant foam, and shaving foam.

1.2 Oil Field Applications

In the oil and gas industry, foams are used for a range of applications such as drilling, enhanced oil recovery (EOR), hydraulic fracturing, cementing, and stimulation amongst others. In refineries, unwanted foams form in distillation towers and oil-gas separators, which must be chemically broken down into their constituent chemicals. Foams are widely used because of their unique properties such as high viscosity and low density, which make them suitable for hole cleaning and downhole pressure management. In addition to their high viscosity, the bubble

structure of the foam plays a vital role in increasing their carrying capacity. In field applications, the foam generated has a foam quality of 90% when measured at surface but the foam quality reduces in downhole conditions due change in pressure and temperature.

1.1.1 Drilling

Formation damage is one of the leading causes of poor well performance (Falk and McDonald 1995). Underbalanced drilling with lightweight drilling fluid-like foam improves the rate of penetration, reduces formation damage with minimal or no stimulation required, reduces chances of differential pipe sticking, minimizes lost circulation, and faster payback due to production of formation fluids while drilling (Capo et al. 2006). Foam drilling is highly beneficial for water-sensitive formations and regions with water shortages. The use of high-quality foams with appropriate flow rate ensures good hole cleaning for inclined and horizontal wells (Martins et al. 2001). When applied for drilling in depleted zones and low-pressure formations, foams are more cost-effective than traditional fluids because they halt fluid leak off into the formation, reducing fluid loss and the amount of drilling fluid used.

1.1.2 Hydraulic Fracturing and Stimulation

Fracturing occurs when the wellbore pressure exceeds the formation's pore and overburden pressures and. Foams exhibits properties that are suitable for fracturing applications such as low fluid loss, high proppant carrying capacity, low hydrostatic head, quick fluid recovery, low formation damage, exceptional flow back, and good wellbore cleanout capability (Kumar et al. 2010; Blauer and Kohlhaas 1974). Frequently, foam fracturing is implemented in low permeability gas reservoirs, water-sensitive shale formations, coalbed, tight sandstones, and carbonates. The fluid used in the fracturing consists of 65-85% of the gaseous phase which is mostly made up of either nitrogen, carbon dioxide, or natural gas. The foam's high gas content

aids in the rapid return of liquids in the form of mist. In addition, good post-treatment viscosity-breaking characteristics elevate the use of foam as fracturing fluid. Also, recent acid stimulation studies show that Nano surfactants are better suited for higher temperature applications (Omar et al. 2018).

1.1.3 Enhanced oil recovery

Enhanced oil recovery is a technique for increasing output in wells that have reached their inherent capacity for oil production. Carbon dioxide gas is the most widely used fluid for EOR along with nitrogen, hydrocarbons, air, and water (Worthen et al. 2012). These fluids are less successful in dislodging hydrocarbons from the pore space in the reservoir due to their low density and viscosity. The flowing of foam as an EOR fluid through the porous media is unique because its rheology and microstructure (Kovscek and Radke 1994). The ability of an aqueous foam stabilized with a surfactant to limit gas mobility in porous media which increases the sweep efficiency (Fried 1961). The gas mobility reduction factor is dependent on the surfactant concentration and injection velocities (Simjoo et al. 2013). Recent studies show that nano particle-stabilized carbon dioxide foams show greater efficiency in reducing gas mobility in gas-injected EOR (Ortiz et al. 2018). An optimized mixture of nitrogen and carbon dioxide for generating foams increases the recovery of oil when compared to recovery by pure carbon dioxide foams (Gajbhiye 2021).

1.1.4 Cementing

Foam cement is employed when lower slurry densities are required for long-term performance in high-pressure, high-temperature zones (Ahmed et al. 2008). When the casing is pressured, foamed cement deforms but does not crack like conventional cement. Foamed cement slurries have superior displacement properties due to their high viscosity providing good zonal isolation.

The low thermal conductivity of nitrogen foamed cement allows less heat to escape the casing boundary (Benge et al. 1982). Resistance to impact and cyclic loading improved due to improved physical and mechanical properties. Foam cement works well for cementing wells with lost circulation issues and removes the need for multi-stage cementing procedures, saving time and money (Peskunowicz and Bour 1987).

1.2 Problem Statement

Although foam has many applications in the oil and gas sector, it is thermodynamically unstable fluid. Properties of foam such as low density and high viscosity are extremely critical but deteriorate with time. Foams have high sand carrying capacity which is due to their bubble structure. Therefore, it is necessary to have a better understanding of foam's rheology, drainage, stability, bubble size, and hydraulics. In downhole conditions, foam is affected by the presence of contaminants like oil, salt, clay, and several other impurities. The effects of pressure and temperature on various foam characteristics must be thoroughly investigated. The quality of foam has a major influence on the foam properties and changes with temperature and pressure.

Gravitational drainage, bubble coalescence, and Ostwald ripening all contribute to foam decay. The difference in density between the liquid and gas phases is the driving mechanism that causes gravity drainage. The walls of the bubbles get thinner as the liquid drains from the foam structure. Surfactants, on the other hand, slow down film thinning, a phenomenon known as the Gibbs-Marangoni effect (Zhou et al. 2020). Coalescence (Fig.1.1) of two bubbles in the foam structure to form a larger bubble destabilizes the foam structure as larger bubbles are unstable. Gas migration from smaller bubbles to bigger bubbles is known as Ostwald ripening.

With increasing depth, downhole circumstances vary, affecting the downhole conditions for foam flowing through the annulus. In past few years, drilling inclined wells has increased and

research showed that well inclination speeds up the drainage process (Govindu et al. 2021). Aqueous foams have demonstrated promising outcomes in geothermal drilling applications where lost circulation is a problem, but only at temperatures below 70°C. The bubble structure of aqueous foams breaks down at high temperatures, hence they can't be used at elevated temperatures.

High-quality aqueous foams show a hexagonal bubble structure, and low-quality foams display a normal spherical structure (Fig. 2.2). The average bubble size increases with time as the foam decays due to coalescence and coarsening, and consequently, the number of bubbles decreases with time.

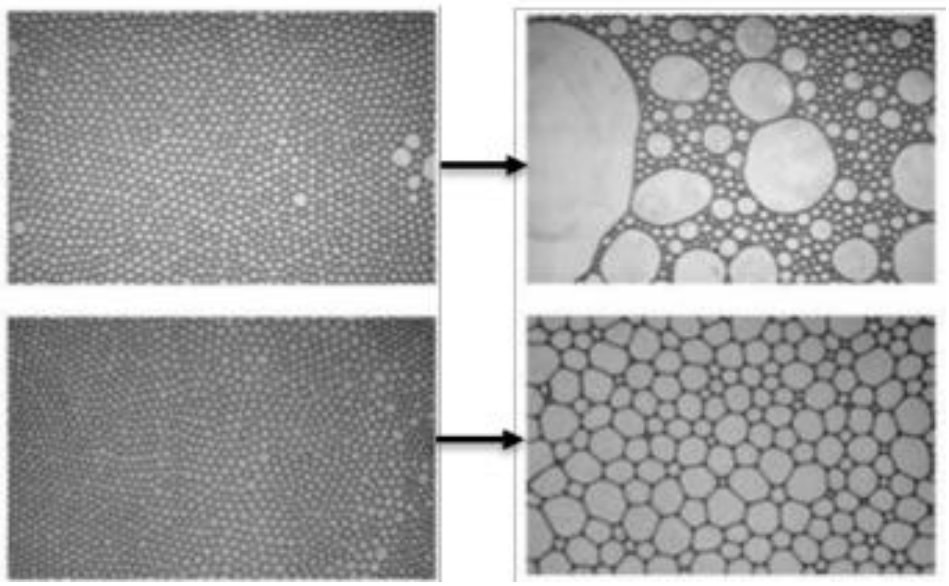

Figure 1.1: Coalescence (top) and coarsening (bottom) (Hill and Eastoe 2017)

The application of oil-based drilling foams is limited due to environmental concerns. Using unstable aqueous foams for underbalanced drilling can cause temporary overbalance conditions, causing severe formation damage. Therefore, it is necessary to understand the drainage, rheology, and stability of aqueous foams.

1.3 Objectives & Scope of work

The principal aim of this investigation to understand the drainage behavior and the half-life of oil-contaminated aqueous foams under various conditions, including different pressures and foam qualities. The specific goals of this investigation include:

- Studying the effects of pressure and oil contamination on the bubble size distribution and drainage behavior of foams.
- Examining the impact of pressure on the mechanism of foam drainage in the presence of contaminant oil.
- Investigating the impact of oil contamination on the structure of foam under various conditions.
- Developing correlations to relate to foam drainage and half-life to it is characteristics such as bubble size distribution, foam quality, and pressure.

The scope of the current study is focused on the experimental investigation of the drainage of aqueous foam in the presence of oil contaminants and different pressures. Therefore, aqueous nitrogen foams used in this study were tested with varying test parameters such as quality, pressure, and oil concentration. Foam quality and pressure were varied between 40-60%, and 100-400 psi. Oil contaminant concentration was from 0 to 20%. Bubble size and structure are studied in order to understand the drainage of aqueous foams. The quality of foam was regulated by adjusting liquid injected into the system, which was done in a closed-loop system. In the liquid mixture, a 2% concentration of anionic surfactant was added.

1.4 Properties of Foams

Foam has a number of useful properties that have been stated previously, allowing its utilization in a variety of applications. These properties largely depend on the method of foam generation, type of surfactant, properties of base fluid, pressure, temperature, and contaminants present in the fluid system. Some of the important properties of foam are discussed in this section.

1.4.1 Quality

The foam quality is the in-situ volumetric concentration of the gas phase present in the foam. It is one of the most essential characteristics that gives foam its distinctive attributes. Foam quality affects the stability, viscosity, bubble size distribution, and structure of foams. Foam quality is mathematically defined as the ratio of the in-situ volume of gas to the total foam volume:

$$\Gamma\,(\mathrm{T},\mathrm{P}) = \frac{V_G}{V_G+V_L} \tag{1.1}$$

Where V_G and V_L are volume of gas (V_G) and volume of liquid (V_L), respectively. The in-situ gas volume varies with pressure and temperature; as a result, foam quality is a function of pressure and temperature.

As the foam quality is increased from zero to unity, we see a transition in the foam structure (Fig. 1.2). Foams below 60% are identified as bubbly liquids. For aqueous foams, rigidity transition occurs at 63% (Kraynik 1983; Ahmed et al. 2003). Foams above 96% are classified as mists. Wet foams have high liquid content than dry foams. Due to thicker films, wet foams have a spherical structure and dry foams have thinner films with polyhedral structure. Foam density is majorly influenced by the change in density of the base fluid as change in gas density has negligible effect. The density of the foam structure changes with the foam quality. Foam density is calculated as a mixture of density of gas and liquid. As the quality of foam gets

higher, the fraction of liquid present in the foam structure reduces and the fraction of gas present in the foam structure reduces. The drainage of the liquid phase from the foam structure reduces the amount of liquid and thus reducing the overall density of foam drastically.

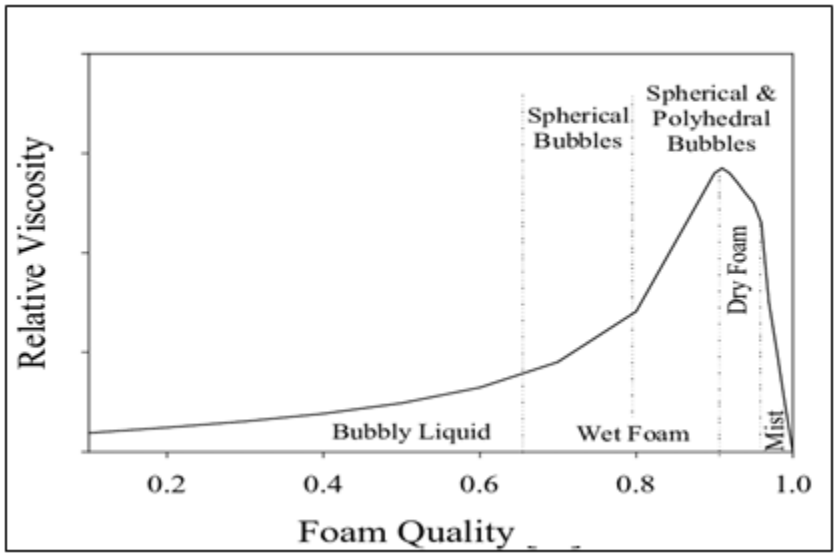

Figure 1.2: Relative viscosity as a function of foam quality (Ahmed et al. 2003)

1.4.2 Rheology

The rheology of the foam is determined by the quality of the foam and the base liquid viscosity (Sherif et al. 2016; Mitchell 1971). The shear rate that is applied to the foam influences its rheology, while surfactant concentration has a slight effect. The liquid used is usually oil, water, or polymer with a gas phase consisting of nitrogen, carbon dioxide, or hydrocarbons. Wet foams made with these fluid mixtures exhibit Newtonian behavior. As the quality increases, non-Newtonian, pseudoplastic fluid behavior also increases. Besides this, foam rheology is affected by foam generation method, pressure, temperature, and shear rate. Foam made of a high-viscosity liquid phase often exhibits higher stability because the viscous force impedes liquid movement and opposes drainage. The viscosity of non-dry foam increases with quality.

1.4.3 Stability

Foams exhibit unique properties, but they start to drain and lose their properties as soon as they are created. Foam's stability is mainly influenced by its quality and base liquid rheological properties. Foams with higher qualities are found to be more stable. Wet foams decay faster than dry foams. The stability of foams is measured as the drainage of fluid from the foam structure. Drainage in foam occurs by gravitational drainage, coalescence, coarsening, and Ostwald ripening. As the liquid drains from the foam structure, the walls of the bubble become thinner and unstable. Furthermore, bubble size and structure impact foam stability. Foams containing bubbles of small size are proved to be more stable than foams with large bubbles. In dry foams, bubbles are so tightly packed that they start impacting the neighboring bubbles such that they take a polyhedral shape. The addition of surfactants increases foam stability by lowering the surface tension. However, increasing surfactant concentration beyond critical micelle concentrations does not improve the stability of foam.

1.5 Factors Affecting the Foam Stability

Foam stability is mainly a function of its quality and base liquid rheology as mentioned earlier. Other factors that have effects on foam stability are pressure, temperature, contaminants, surfactant type, and foam generation techniques.

1.5.1 Effect of Pressure

An increase in pressure at a constant foam quality doesn't have significant effect on the foam viscosity (Lourenco et al. 2003; Akhtar 2017; Akhtar et al. 2018). Experiments conducted with various surfactant types and gas combinations show that drainage time increases with pressure (Rand and Kraynik 1983). The improvement in drainage time at a constant quality can be linked

to the decrease in bubble size (Rand and Kraynik 1983). The change is the size of the bubbles is attributed to the compressibility of gas phase (Fig. 1.3).

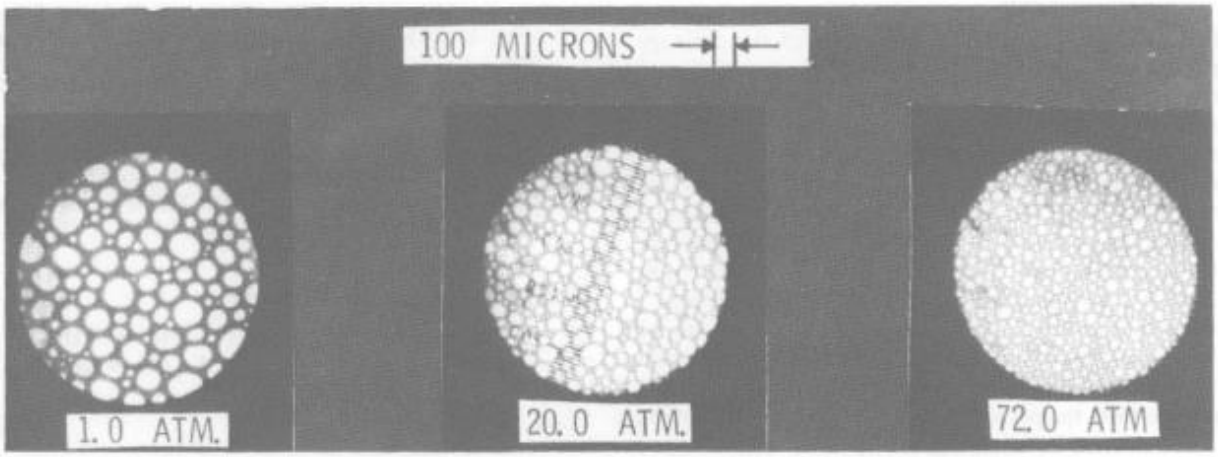

Figure 1.3: Microscopic images of bubble size with varying pressure (Rand and Kraynik 1983)

An increase in pressure reduces the bubble size and creates a uniform foam texture. This uniform texture of the foam slows down the drainage and decay of the foam structure. Increasing pressure at constant foam quality affects foam stability by modifying surface elasticity (Ruckenstein and Jain 1974). This improved surface elasticity prevents rupture of thin films and delays bubble coalescence. Moreover, when compared to anionic surfactant foam, amine oxide surfactant foam exhibited higher stability and delayed foam drainage when pressure was increased (Fuseni et al. 2014). Also, foam flooding experiments demonstrated that foam stability increases with increasing pressure (Holt et al. 1996). However, extremely high-pressure conditions might cause the lamella to rupture and destabilize the foam (Sheng 2013).

1.5.2 Effect of Temperature

Increasing temperature can affect gas phase volume, foam quality, pressure, and viscosity of the base liquid. When quality is kept constant, the apparent viscosity of foam decreases significantly with temperature (Akhtar 2017). The reduction is mainly due to thermal thinning of the base

liquid. Effect of temperature on foam viscosity is more pronounced in high-quality foams (Gu and Mohanty 2015). Foams swell with increase in temperature which is due to the expansion of gas phase in foams. When the temperature of foam is increased, foam volume reaches a peak value after which the foam volume decreases due to the evaporation of water from the foam structure (Li et al. 2012). Presence of solid particles increases the drainage rate initially and decreases later. Increase in temperature, rapidly decreases foam height in a static foam drainage test (Wei et al. 2020). Surfactants that are stable at high temperatures are used for creating stable foams at high temperatures. The addition of surface-modified nanoparticles increases the stability of aqueous foams at high temperatures (Singh and Mohanty 2017, Zhu et al. 2017).

1.5.3 Effect of Contaminants

As drilling or completion foam circulates in the wellbore, it encounters contaminants like salt, oil, and clay. Lower concentrations of salt like NaCl and $CaCl_2$ stabilize the foam. However, at higher concentrations, they destabilize the foams across all qualities (Obisesan et al. 2020). The effect of oil on the stability of foams is sensitive to foam qualities. At lower qualities, the presence of oil helps increase the stability of foams but as the foam quality increases above 60% the foam becomes unstable (Obisesan 2021). Clays like bentonite and kaolinite improve the stability of foam at all qualities with increasing clay concentrations (Obisesan 2021).

1.5.4 Effect of Additives

Foam stabilizing agents like fiber, polymer, and nanoparticles have been used to attain higher stability in foam structures. Nano particles along with surfactants provide stability to foam structure in presence of oil and salt (Qian et al. 2020). This is due to the change in curvature of lamella boundary and forming a barrier to minimize the contact area between bubbles which reduces the foam destabilizing process. Bentonite nanoparticles stabilize the foam and make

them resistant to temperature and oil (Zhu et al. 2017). Fly-ash nanoparticles are inexpensive, and an exceedingly small amount of these nanoparticles show higher stability in presence of oil (Eftekhari et al. 2015). Addition of polymers improves the quality of foam and multiplies the half-life period and foam stability (Zvada et al. 2021). Sodium dodecyl sulfate surfactant with hydroxyethyl cellulose polymer is less stable as compared to their combination with nano silica (Parvaneh et al. 2022).

1.5.5 Surfactant Type

Surfactants lower the surface tension between the liquid phase and gas phase and stabilize the interface between the two phases created when the foam is generated by mixing or shearing. Experimenting with different surfactant types like anionic, amphoteric, cationic, and non-ionic showed that anionic surfactants take the highest time to reach half-life (Rand and Kraynik 1983). Besides this, recent studies show that nanoparticles and nano surfactants are better suited at higher temperatures (Omar et al. 2018, Singh and Mohanty 2017).

1.5.6 Foam Generation Techniques

The primary requirements for aqueous foam generation is the presence of water containing a surface-active agent and mixing mechanisms. The method by which the foam is generated affects its properties. The bubble size distribution, rheological characteristics, drainage behavior, and half-life affected by foam generation technique. Different sizes of the mesh have been used to generate foam (Harris 1989). One of the methods includes in-situ generation of foam using a rotary mixer. Other methods used for generating foam involve the use of orifices, needle valves, and liquid phase vaporization.

2. CHAPTER TWO

Literature review

Foam is a multiphase fluid that exhibits instability affected by various factors. Quality and base-liquid viscosity are foam properties that directly impact its stability. Pressure, temperature, and contaminants can influence foam stability indirectly. Therefore, foam stability at high-pressure and high-temperature conditions is essential in underbalanced drilling.

Oil is one of the most common downhole contaminants. Often foam drainage rate changes with the oil concentration in the base liquid (Obisesan 2021). Contaminants like oil can influence foam structure and bubble size distribution that are instrumental in determining the characterization of foams. Bubbles of various sizes and structures can be produced using different foam generation techniques and surfactants (Ozbayoglu 2005).

2.1 Foam Structure and Bubble Size

Properties of aqueous foams are related to their bubble structure. For a given quality, foam structure is determined by the minimization of surface energy. Plateau borders are edges formed when three bubble walls meet (Thomas et al. 2015). In 19^{th} century, a Belgian physicist Joseph Plateau established some fundamentals, known as Plateau's laws (Plateau 1873). It states the followings:

a. Thin films are smooth and have a constant mean curvature
b. At the Plateau border, three films join together at an angle of 120°
c. The Plateau borders that link at one point come in a group of four and at an angle of 109.5 in a tetrahedral geometry (Fig. 2.1).

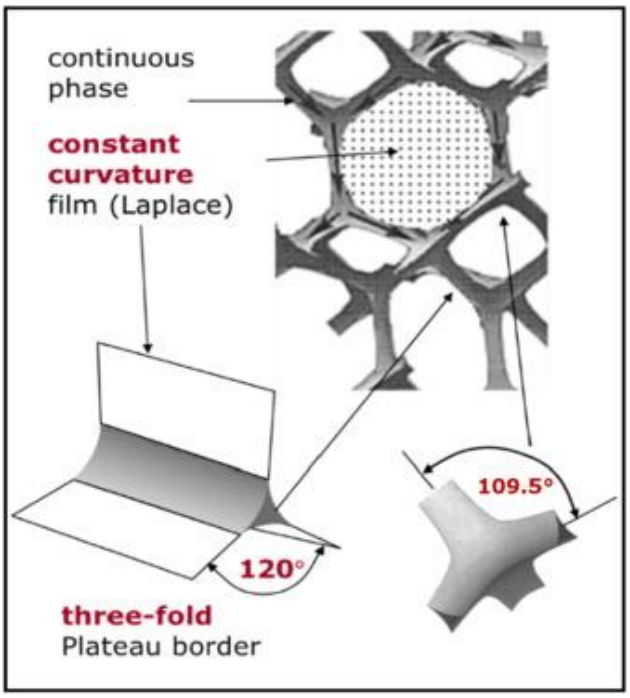

Figure 2.1: Geometry and topology of aqueous foam at high qualities (Drenckhan and Hutzler 2015)

Bubble shape and structure depend on the foam quality (Drenckhan and Hutzler 2015). Bubble size increases with the gas volume fraction, more gas in the system means higher the bubble size. The bubbles get their opacity from the dispersion of light from the liquid film surface and plateau borders. Small bubbles scatter more light, thus making the foam appear whiter. An example of this is shaving foam and whipped cream.

2.1.1 Aqueous Foams

High-quality aqueous foams show a hexagonal bubble structure, and low-quality foams display a normal spherical structure (Fig. 2.2). The average bubble size increases with time as the foam decays due to coalescence and coarsening, and consequently, the number of bubbles decreases with time.

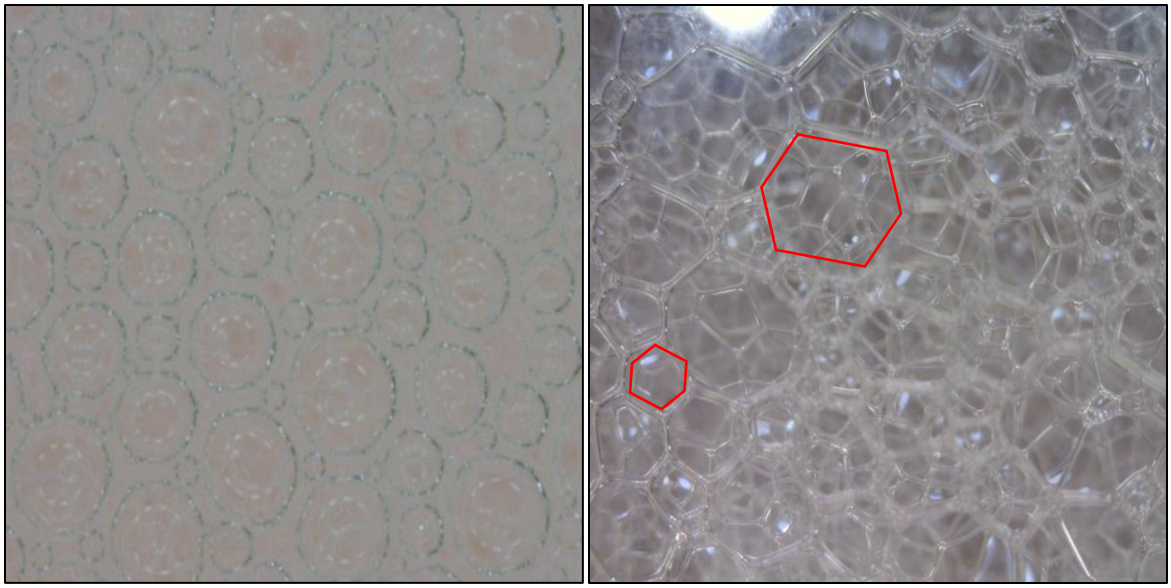

Figure 2.2: Spherical structure of aqueous foam at low quality (Left) and Polyhedral structure of aqueous foams at high quality (Right)

The surface tension acting on the bubbles is given by the Young – Laplace law as excess pressure of a bubble inside a liquid is given by surface tension, and radius of bubble, R. Thus:

$$\Delta P = 2\gamma/R \tag{2.1}$$

And the energy of the foam for n bubbles is given by:

$$E = \gamma \sum_{i=1}^{n} S_i = \gamma\, S_{total} \tag{2.2}$$

For a bubble of size of 100 µm, the surface energy is about 10^{13} times higher than the thermal energy which means that surface energy dominates the bubble packing over thermal energy (Drenckhan and Hutzler 2015). Thermal energy is the total internal kinetic energy of an object due to the random motion of its atoms and molecules. The average bubble size is smaller at the bottom of the foam structure because the foam at the bottom is wet foam, and the average bubble size is larger at the top of the foam structure because the foam at the top is dry foam.

2.1.2 Oil-Contaminated Foams

For aqueous foams, oil acts as a contaminant but doesn't enter the bubbles. Oil droplets travel through the foam lamella overcoming the electrostatic interactions (Telmadarreie and Trivedi 2018). As the oil droplet approaches the gas-liquid interface, it forms an oil film at the gas interface called a pseudo emulsion film. Oil droplets cannot penetrate the bubble when the pseud emulsion film is stable. The presence of vesicles creates a thick film around the bubbles (Fig. 2.3) and contributes to the slowing down of the coarsening of bubbles (Rio et al. 2014).

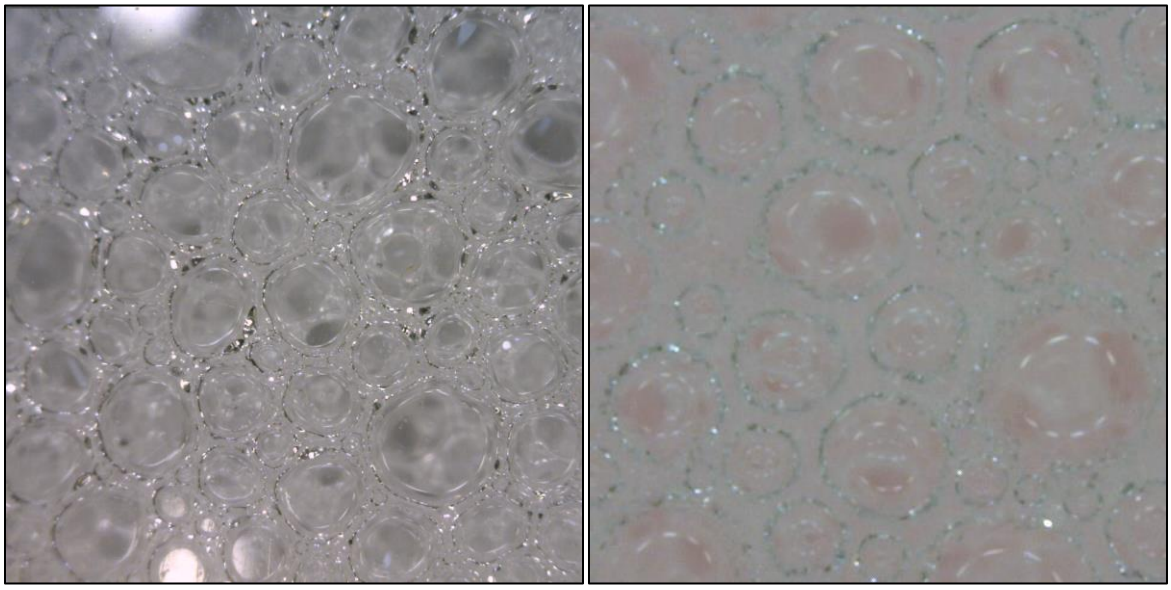

Figure 2.3: Spherical structure of aqueous foam at an early stage (Left) and after 5 minutes (Right)

Oil-laden foams have a fragile structure and lose their pseudo emulsion property easily. Small oil droplets get trapped in between the plateau borders. Small oil globules come together to form big oil globules which deform the plateau border and destabilize the foam (Mensire and Lorenceau 2017). This process is also accelerated by drainage of liquid phase making bubble films thinner.

2.2 Drainage Mechanism

Foam structures are a part of non-equilibrium systems like emulsions or off-critical decomposing mixtures that change their shape and size with time (Carrier and Colin 2003). Foam destabilization can be explained by two methods: drainage and decay. Drainage is the loss of the liquid phase from the foam structure and is governed by capillary and gravitational forces. During foam decay, there is a loss of bubbles in the foam structure due to the merger of smaller bubbles into larger bubbles known as coarsening and bubble coalescence which is caused by the rupturing of the bubble film. In this study, the stability of aqueous foams is studied by measuring the drainage with respect to time. Foam drainage occurs because the trapped foam has a natural tendency to acquire static equilibrium. Constant drainage and decay cause changes in foam structure and thus alter the property of foam continuously (Cohen et al. 2015). Therefore, it is necessary to understand the drainage mechanism of the liquid phase in the foam structure.

There are three drainage regimes in static foam columns (Fig. 2.4). In Regime 1, the drainage rate is transient and increases rapidly. After that, the drainage due to gravity is countered by viscous and capillary forces, which establish an equilibrium between them, and the drainage rate becomes constant represented in Regime 2. As the gravitational drainage increases, the amount of liquid fraction present in the foam structure decreases. This causes the liquid film to become thin and stop further drainage. In Regime 3, foam decaying is dominated by coalescence and coarsening as the foam film structure dries.

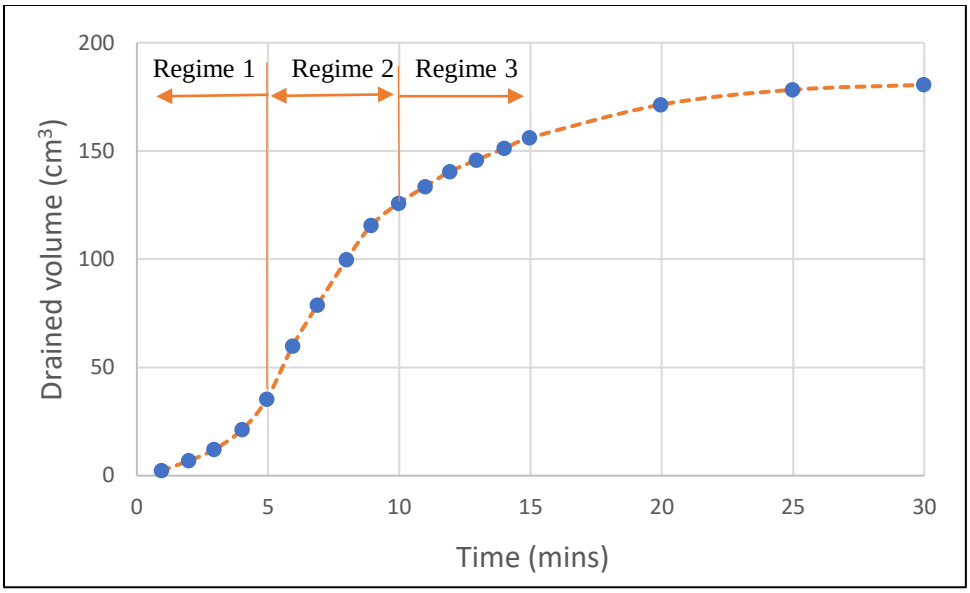

Figure 2.4: Foam drainage curve (Redrawn using data from Agrillier et al. 1998)

When foam is directly exposed to the atmosphere without any covering, the liquid film evaporates from the top surface and accelerates the drainage process. The larger bubbles rise to the top of the foam structure as they have a large gaseous phase entrapped in them decreasing the overall density of the bubbles. The presence of fatty alcohols and oil on the film surface reduces the rate of water evaporation significantly (Barnes 1986). For a trapped foam, conventional drainage occurs through the plateau borders.

Gravitational Drainage: Foam drainage can be explained as the flow of liquid through the plateau borders and nodes between bubble structures which is induced by gravity. Moreover, bubbles with large volumes rise quickly due to the buoyancy and the heavier liquid is collected at the bottom of the foam column. This phase-based segregation phenomenon is called Gravitational Drainage. As foam quality increases from 70% due to drainage, the bubble change from spherical to polyhedral. Close examination of the drainage process indicated that the maximum drainage occurs at the interconnected network of Plateau borders (Cohen et al. 2015). One of the crucial factors for gravity drainage is the coupling of bulk and surface flows at

plateau borders and nodes, which can be adjusted by the surfactant and base liquid viscosity (Saint-Jalmes 2006). Drainage time can be defined as the period of liquid drainage from the foam structure driven by gravity until an equilibrium state is found between the capillary effects and gravity. Basic foam drainage model was introduced by (Kraynik 1983) where simplifying assumptions were made to reduce the number of parameters. Assumptions made were:

1) Rigid gas-liquid interface
2) Uniform Initial liquid volume fraction distribution
3) Liquid hold-up in the films is negligible

Foam drainage time-dependent model was modified by (Koehler et al. 1998; Koehler et al. 2000):

$$T_{drain} = \frac{H\eta}{K\rho g R_{avg}^2 \Phi^{\alpha}} \tag{2.3}$$

where H is the foam height, R the average bubble radius, ρ is liquid density, η is viscosity, g is acceleration due to gravity, K is dimensionless permeability and α is an exponent between 0.5 and 1. This model is effective for wet foams and the drainage time for dry foams is negligible. K and α depend on the mobility of the surface layers protecting the bubbles which again depends on compression modulus and surface shear viscosity (Saint-Jalmes et al. 2004). Foam drainage can be stopped if the liquid phase manages to solidify or form a gel.

Coarsening: Foams attain their thermodynamic equilibrium by reducing total surface area as the average size of the bubbles increases with time and coarsening of bubbles occurs (Hilgenfeldt et al. 2001). Coarsening is a process that involves the movement of the gas phase from smaller bubbles to larger bubbles increasing the average bubble radius. The Laplace pressure is the driving mechanism for this process. Laplace pressure is the pressure difference between the

curved surface or interface. This pressure jump arises due to surface tension or interfacial tension, which compresses the curved surface or interface. Coarsening follows the same principle as the phenomenon of Ostwald Ripening (Rio et al. 2014). The diffusion of gas happens through the thin film between the bubbles as it provides the smallest diffusion path. The gas's effective diffusion coefficient (D_{eff}) and nature are the driving factors for the characteristic coarsening time. The coarsening effect becomes significant when the drainage curve reaches the plateau region and the period through which this coarsening effect lasts is called as coarsening time. Coarsening time is given by (Hilgenfeldt et al. 2001):

$$T_{caors} = \frac{R_{avg}^2}{D_{eff} f(\phi) h} \tag{2.4}$$

Coarsening time is observed as foams get drier and the liquid fraction is less than 0.36. Highly soluble gases such as carbon dioxide crate less stable foam because they dissolve in water and quickly diffuse through the thin film between the bubbles. The diffusion of gas can be slowed down by using less soluble gas like nitrogen instead of carbon dioxide (Weaire and Pageron 1990). Consequently, strong coarsening of bubbles causes faster liquid film drainage and foam degradation.

Coalescence: As the bubble structure attains equilibrium from the drainage and reaches a critical liquid volume fraction, the bubble films become thin and rupture. This process leads to bubble coalescence. Unlike coarsening, there is no diffusion of gas in coalescence. Due to rupturing of the bubble film, there is a loss of gas in the foam structure. Bubbles coalescence can be reduced by adding stabilizing agents like polymers, nanoparticles, proteins, low molecular weight surfactants, or their mixtures (Tcholakova et al. 2008).

2.2.1 Aqueous Foams

The drainage process of foams in vertical columns can be explained by considering different natural phenomena. As the foam quality increases the drainage rate decreases. This is due to the increase of viscous force as the foam quality increases and liquid fraction decreases (Kruglyakov et al. 2008). The foam becomes dry, and the bubble films become thin. As the film becomes thin, the area of flow through the conduit decreases, and the effect of capillary and viscous forces increases which hinders the drainage of dry foams.

The drainage in inclined columns is more complex due to the presence of lateral drainage along with vertical drainage (Fig. 2.5). The lateral drainage results in forming a liquid layer on the low side of the column. Due to gravity, the liquid layer flows downward in the inclined wall and accumulates at the bottom of the column. As a result, a higher drainage rate is observed in the inclined column than in a vertical one (Govindu et al. 2021).

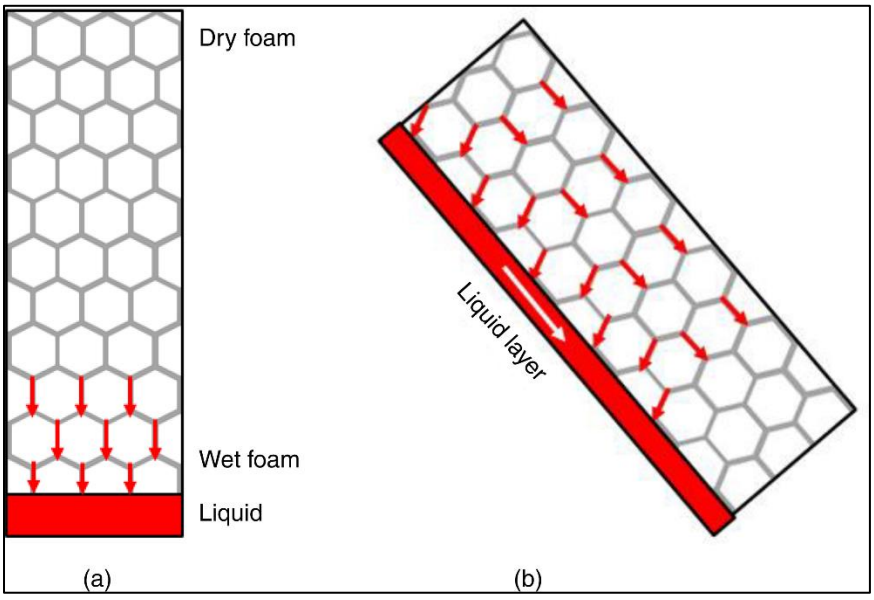

Figure 2.5: (a) Drainage in Vertical column (b) Drainage in Inclined column (Govindu et al. 2021)

2.2.2 Oil-Contaminated Foams

Foams show certain change in stability in presence of oil due to the interaction of contact phases between the oil phase and the porous phase of the foam structure (Schramm and Novosad 1992). Based on oil types in foam emulsions, there are three types of foam A, B, and C (Fig. 2.6) respectively as described by (Schramm and Novosad 1990). These foams can be classified on the basis of Lamella number. Lamella number is a dimensionless ratio of pressure drop between the plateau border and oil drop. Lamella number is calculated by:

$$L = \frac{\Delta P_c}{\Delta P_R} = \frac{\gamma_F / r_p}{\gamma_{OF} / r_o} \tag{2.5}$$

Where, ΔP_c = Pressure drop at the plateau border

ΔP_R = Pressure drop at the oil-foam interface

Υ_F = Foaming aqueous solution surface tension

Υ_{OF} = Foaming aqueous solution/oil interfacial tension

r_p = Radius at plateau border

r_o = Radius of the oil drop

Later they found experimentally that the ratio of r_o/r_p is 0.15 (Schramm and Novosad 1992).

$$L = 0.15 \frac{\gamma_F}{\gamma_{OF}} \tag{2.6}$$

Type A foams have L values less than unity. Type B foams exhibit L values ranging between 1 to 7, whereas Type C foams have L values greater than seven. Type A foams are the most stable in the presence of oil, and Type B and C foams become less stable with the increasing Lamella number.

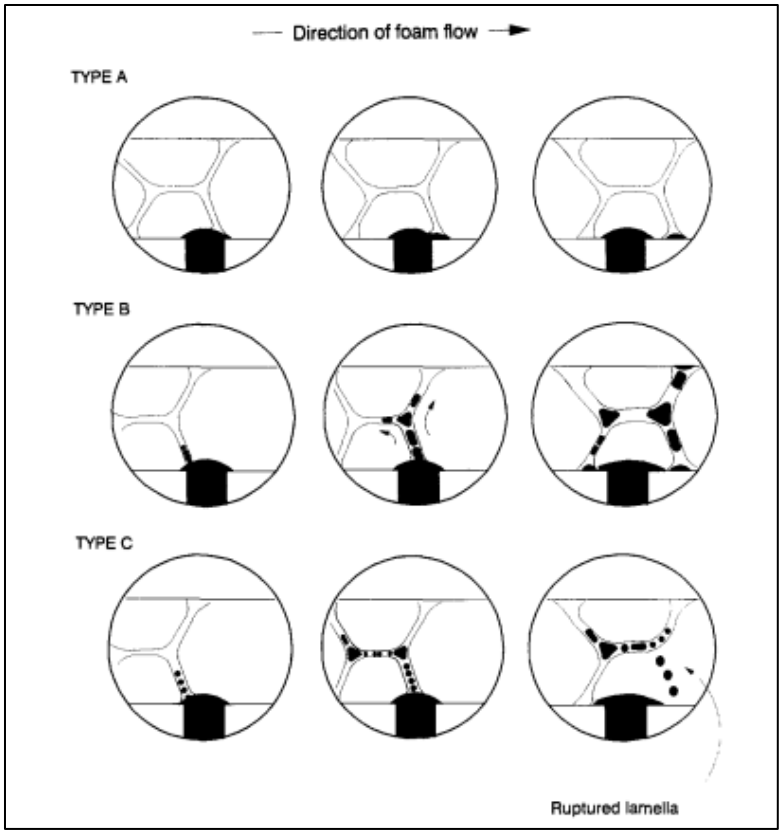

Figure 2.6: Types of foam and their behavior after oil contact (Schramm and Novosad 1990)

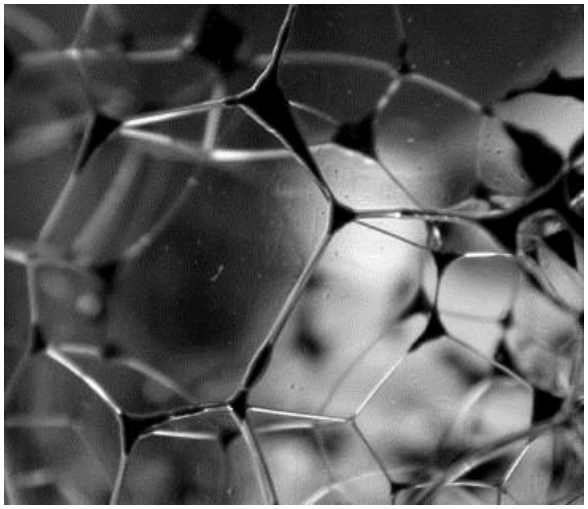

Figure 2.7: Oil particles trapped at the Plateau borders and nodes for 5% oil v/v (Vikingstad et al. 2005)

It is found that the stability of the foams with emulsified oil depends on the stability of the pseudo emulsion film that forms between oil and the gas-liquid interface (Koczo et al. 1991). If

the pseudo emulsion film is stable, the oil does not enter the gas-liquid interface (Fig. 2.7) but if it is unstable then the oil droplets enter the bubble and destabilize the foam.

2.3 Foam Drainage Models

Foam drainage is studied over a macroscopic scale so that a continuum or coarse-grained approach is appropriate. Foam drainage is the flow of the liquid phase from the foam structure through interstitial spaces between the bubbles. The interstitial flow can be through three different ways:

a. Films formed between two neighboring bubbles that have almost flat bubble faces.
b. Plateau borders, where three films meet.
c. Nodes or junctions, where four plateau borders intersect.

Foam drainage models have been developed based on conservation laws as they can help predict the drainage characteristics of foams under various conditions. Various foam drainage models have been developed to predict foam quality profile during the drainage process. The models for node-dominated and channel nominated drainage are established by applying Darcy's law to foam (Koehler et al. 2000). While deriving the general foam drainage equations, the following assumptions are made.

(a) All bubbles present in the foam structure are monodispersed.
(b) The gas pressure and volume are constant across all bubbles
(c) Compression due to gravity is negligible due to the small weight of the foams.
(d) There is the no-slip interface boundary condition at the walls of the container
(e) The viscosity is assumed to be constant throughout the foam structure

(f) The liquid in the faces is stationary and any motion of channel walls is resisted by the surface viscosity

According to Koehler et al. (2000), the driving force (G) that causes the drainage of foam in vertical configuration is mathematically expressed as:

$$G = \rho g + \nabla(\gamma/r') = \rho g + \frac{\gamma \delta_{\varepsilon}^{1/2}}{L} \nabla \varepsilon^{-1/2} \quad (2.7)$$

Here the first term is the hydrostatic pressure gradient, and second term is pressure gradient due to the surface tension at the boundary. The radius in the second term can be approximated with channel length for dry foams where r<<L and bubbles have a polyhedral structure. G is the pressure gradient driving the flow, ρ is the liquid density, g is acceleration due to gravity, r' is the radius of curvature for channels, Ɛ is liquid volume fraction, ðε is a geometric constant for bubble and L is the channel length

The model considers the contributions of viscous dissipation in channels and nodes of liquid network. The driving force is opposed by the viscous force. Hence, balancing these two forces, the generalized foam drainage equation can be expressed as (Koehler et al. 2000):

$$\mu \frac{\delta \varepsilon}{\delta t} + \rho g . \nabla(k(\varepsilon)\varepsilon) - \frac{\gamma \delta_{\varepsilon}^{\frac{1}{2}}}{L} \nabla . (k(\varepsilon) \nabla \varepsilon^{\frac{1}{2}}) = 0 \quad (2.8)$$

For equation 2.8, there are three forces involved i.e., viscous, gravitational and surface forces respectively. In the model development, foam is treated as a porous medium with a permeability that varies with liquid volume fraction. For channel dominated drainage, the permeability of the foam k(ε) is directly related to the liquid volume fraction by:

$$k(\varepsilon) = K_1 L^2 \varepsilon \tag{2.9}$$

where K_1 is a dimensionless number that depends on the geometry of foam structural units.

For one-dimensional drainage, the drainage equation can be further simplified by considering channel dominated drainage (Koehler et al. 2000). Therefore:

$$\mu \frac{\delta \varepsilon}{\delta t} + K_1 \rho g. L^2 \frac{\delta \varepsilon^2}{\delta z} - \frac{\gamma \delta_\varepsilon^{\frac{1}{2}} K_1 L}{3} \frac{\delta^2 \varepsilon^{3/2}}{\delta z^2} = 0 \tag{2.10}$$

For node dominated drainage, the permeability of the foam is directly related to the square root of the liquid volume fraction. Thus:

$$k(\varepsilon) = K_{1/2} L^2 \varepsilon^{1/2} \tag{2.11}$$

Combining Eqns. (6) and (9), the model for node dominated drainage can be formulated as (Koehler et al. 2000):

$$\mu \frac{\delta \varepsilon}{\delta t} + K_{1/2} \rho g. L^2 \frac{\delta \varepsilon^{3/2}}{\delta z} - \frac{\gamma \delta_\varepsilon^{\frac{1}{2}} K_{1/2} L}{2} \frac{\delta^2 \varepsilon}{\delta z^2} = 0 \tag{2.12}$$

where $K_{1/2}$ is a dimensionless number.

The node dominated drainage equation reproduces results from experiments with good accuracy, but the channel dominated equation fails to do so (Koehler et al. 2000). However, channel dominated model showed better accuracy with protein-based surfactants.

Recently, node-dominated and channel-dominated drainage models have been utilized to simulate laboratory experiments conducted with aqueous foams (Govindu 2019). The numerical foam drainage models were formulated considering the following assumptions:

(a) Bubbles in the foam structure are assumed to be monodispersed.

(b) Drainage is considered to be in vertical model only

(c) Uniform surfactant concentration throughout the vertical section

(d) The bubbles are considered to be maintain a spherical shape.

(e) Geometric constant (∂ε) is assumed to be 0.1711.

(f) Effects of wall slip, and container shape are neglected.

Both the models were tested for aqueous and polymer foams of qualities 40%, 60 % and 80%. These models were unique as they included the effect of change in bubble size distribution as the drainage progresses with time. These models predict the change in liquid volume fraction over time in a static foam column. Since, we are working with aqueous foams, we will discuss the results between the experimental and predicted values of the model.

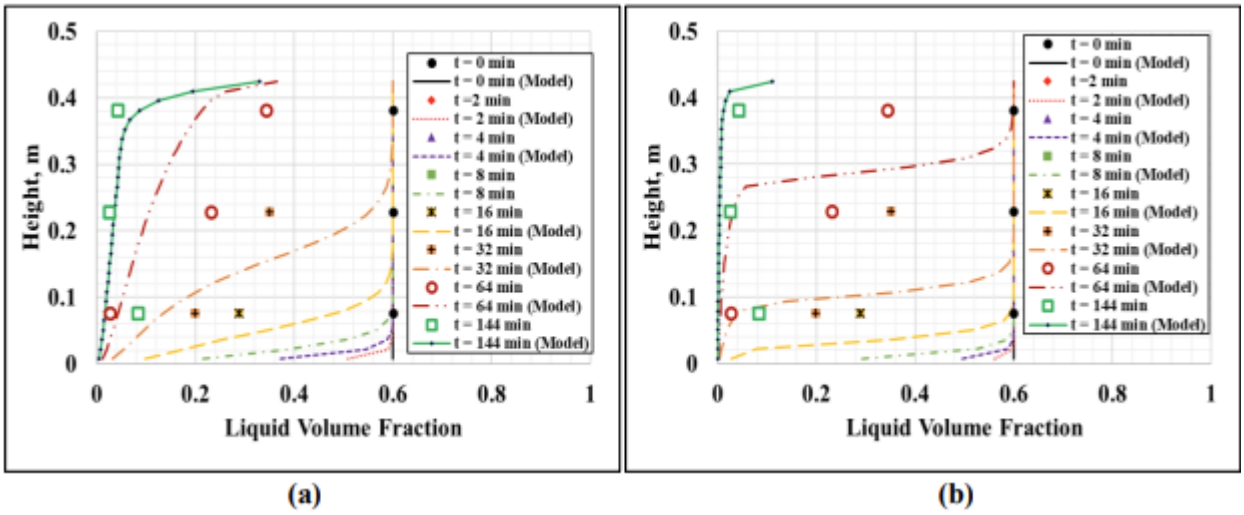

Figure 2.8: Experimental measurements and model predictions for 40% aqueous foams –(a) channel dominated and (b) node dominated models (Govindu 2019)

From (Fig. 2.8) results obtained for 40% quality foams, channel dominated model predicted liquid volume fraction values were slightly off from the values obtained through experimental results. While the node dominated model, over predicted the liquid volume fraction values.

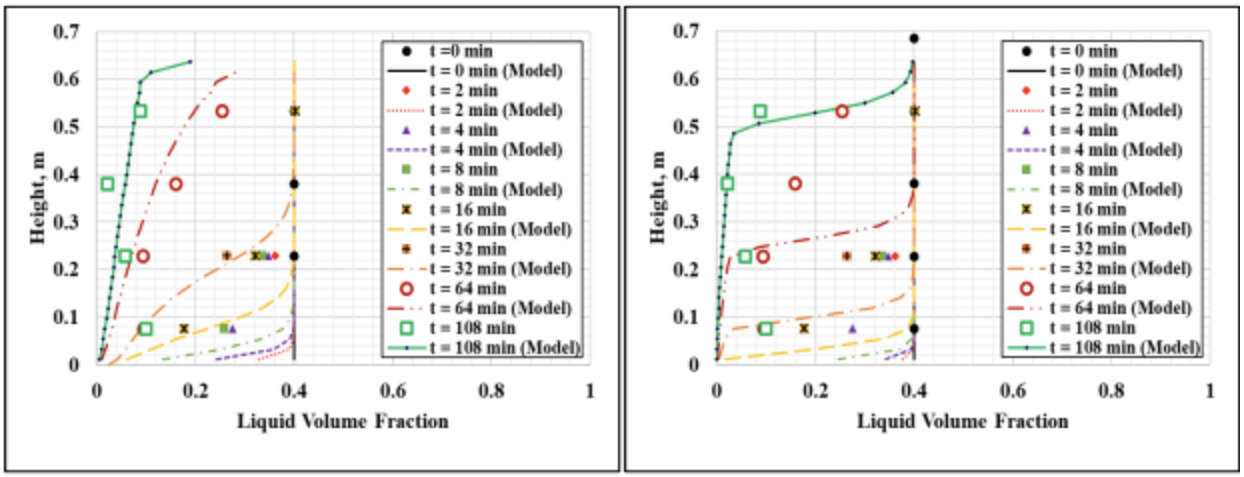

Figure 2.9: Experimental measurements and model predictions for 60% aqueous foams –(a) channel dominated and (b) node dominated models (Govindu 2019)

For 60% foam quality (Fig. 2.9), node dominated models over predicts the liquid volume fraction while the channel dominated model values were closer to the experimental values.

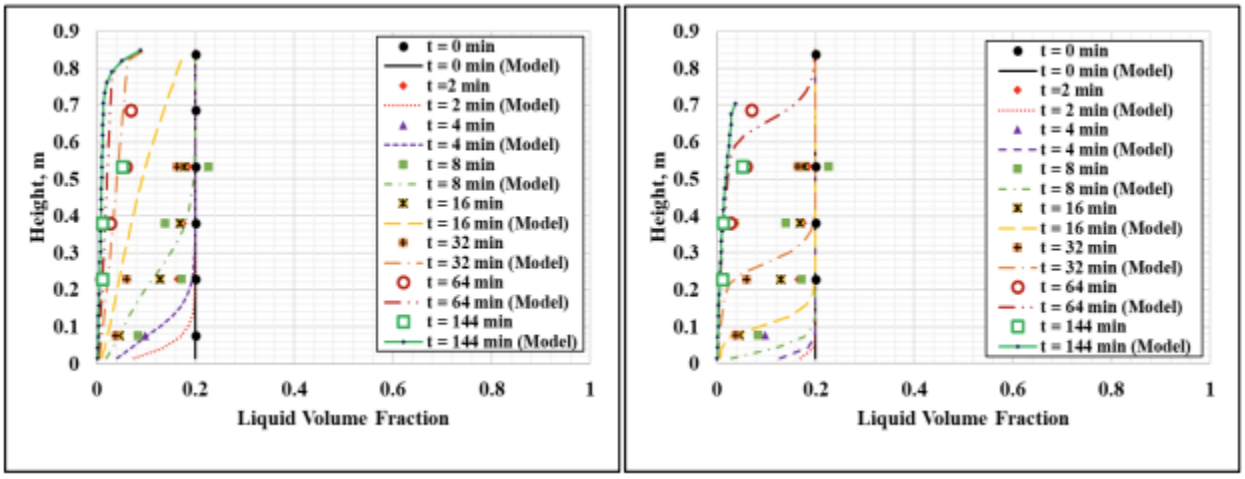

Figure 2.10: Experimental measurements and model predictions for 80% aqueous foams – (a) channel dominated and (b) node dominated models (Govindu 2019)

For 80% foam quality (Fig. 2.10), both the models made decent predictions for liquid volume fraction, however the channel dominated model showed better fit to the experimental values.

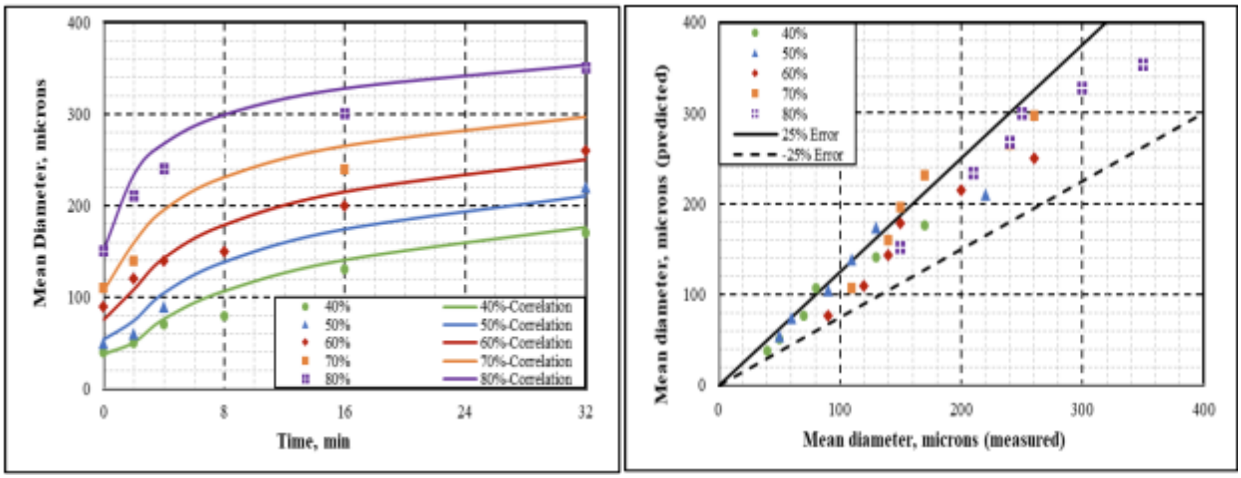

(a) **(b)**

Figure 2.11: (a) Mean bubble diameter correlation for aqueous foams and (b) Error % of correlations (Govindu 2019)

The correlation developed by (Govindu 2019) predicted the average bubble diameter for different foam qualities. However, there were few outliers with these model and majority of the predicted values lie within an error of +/- 25 %. This is because the Non-Newtonian behavior of the liquid phase was not considered.

2.4 Effects of Container Shape

Effects arbitrary container shape on capillarity and vertical gradients are studied and another set of equations were developed by (Saint-Jalmes et al. 2000). Most liquid in the foam structure resides in the random network of plateau borders. So, the average velocity of the liquid in the foam structure can be established by considering the balance of gravity, viscosity, and capillarity:

$$u = u_o \varepsilon^m \left(1 - \sqrt{\frac{\varepsilon_c}{\varepsilon}} \frac{\epsilon}{\varepsilon} \frac{\delta \varepsilon}{\delta z}\right) \tag{2.13}$$

where m is a parameter that depends on the nature of viscous dissipation, u is flow speed, u_o is maximum flow speed, ϵ is capillary rise, ε_c is critical liquid fraction and z is the height of

container. For plateau borders, m = 1, and for vertices, m = 0.5. Assuming that the flow is only downwards, it is easier to deduce a drainage equation for container of any shape. Cross sectional area (A) and height of the container become important parameters to be considered in the analysis (Saint-Jalmes et al. 2000). This:

$$\left[\frac{\delta\varepsilon}{\delta t}+\frac{\delta(u\varepsilon)}{\delta z}\right]+\left[\frac{u\varepsilon}{A}\frac{dA}{dz}\right]=\ 0 \tag{2.14}$$

The first term in the bracket is the drainage equation and the second bracket is accounting for the container shape. For a container shaped like 'Eiffel tower' which flares at the bottom, an exact solution can be obtained (Saint-Jalmes et al. 2000). Therefore, the liquid volume fraction is expressed as a function of position and the time(t) as:

$$\varepsilon(z,t)=\ \varepsilon_o\left(1+\frac{t}{t_o}\right)^{-1/m} \tag{2.15}$$

Here time (t_o) given used in equation 2.16, is given by equation 2.17,

$$t_o = z_o/(u_o\varepsilon_o^m m) \tag{2.16}$$

Where t_o = Initial time, t=0

ε_o = liquid fraction at initial time

z_o = Initial capillary rise

Volume of the corresponding drained liquid is given by (Saint-Jalmes et al. 2000).

$$\frac{V(t)}{V_f}=1-\left(1+\frac{t}{t_o}\right)^{-1/m} \tag{2.17}$$

Where V(t) = Volume of liquid at time 't'

V_f = Final volume of liquid at t = 0

At late time, the model is inaccurate as it doesn't take capillarity and coarsening (Saint-Jalmes et al. 2000).

The fluid velocity is zero at the plateau borders since they are assumed to be rigid. Also, the flow is considered to be Poiseuille-like. For forced drainage model, fluid velocity is given by (Saint-Jalmes et al. 2004):

$$v = K_c^0 \frac{\rho g L^2}{\mu} \varepsilon \tag{2.18a}$$

Here K_c^0 is the dimensionless permeability

But when the plateau borders are not rigid and coupling between bulk and surface flows are taken into consideration. New coupling parameter M is introduced into Eqn. (2.18b). Thus:

$$v = K_c^0 \frac{\rho g L^2}{\mu} (1 + aM^b) \varepsilon \tag{2.18b}$$

The values of a and b are constants varying with liquid fraction. The coupling parameter (M) is defined as:

$$M = \frac{\mu r}{\mu_s} \tag{2.19}$$

Here, μ_s = Surface shear viscosity

A large value of M means more mobility of the surfaces and reduced hydrodynamic resistance of Plateau borders. Another coupling parameter N has been proposed to account for surface tension gradients of bulk and surface flow (Durand and Langevin 2002):

$$N = \frac{\mu D_{eff}}{Er} \tag{2.20}$$

Considering the coupling parameters M and N at the same time, the fluid velocity equation can be written as (Saint-Jalmes et al. 2004):

$$v = \frac{\rho g L^2}{\mu} \varepsilon \left(\frac{1}{\frac{1}{K_c(M,N)} + \sqrt{\varepsilon}/K_n(M,N)} \right) \tag{2.21}$$

The mobility control parameter (M) incorporates bubble size, liquid phase fraction and surface shear viscosity. The importance of this parameter is verified with a large number of experimental data. Hence, the assumption that flow of liquid is through the network of nodes and plateau borders with negligible transport in the thin films is reasonable and it demonstrates the importance of bubble geometries (Koehler et al. 2000). However, this parameter (M) fails for bubbles of small size (less than 0.2 mm diameter) and a bulk-surface coupling parameter N is introduced. For foams drainage with small bubble sizes, the surface mobility is determined by the node and plateau border resistances (Saint-Jalmes et al. 2004).

2.5 Effects of Oil

Foam behavior for oil, gas, and surfactant mixture is characterized by spreading coefficient (Harkins 1941) and entering coefficients (Robinson and Woods 1948).

$$S_o = \gamma_{wg} - \gamma_{wo} - \gamma_{og} \tag{2.22}$$

$$S_w = \gamma_{og} - \gamma_{wo} - \gamma_{wg} \tag{2.23}$$

$$E = \gamma_{wg} + \gamma_{wo} - \gamma_{og} \tag{2.24}$$

Where, Υ_{wg} = Surface tension between water-gas phase

Υ_{wo} = Surface tension between water-oil phase

Υ_{og} = Surface tension between oil-gas phase

A positive entering coefficient means favorable energy for oil to enter the gas-water interface from the water phase side. Negative value of entering coefficient of oil is correlated to the stability of foam. The positive spreading coefficient of aqueous phase on gas-oil interface is an indication of foam stability in presence of oil. Foam stability varies with pressure for different surfactants for both conditions; presence and absence of oil (Holt et al. 1996). Later, it was found that entering and spreading coefficient values are not enough to judge foam's stability, but the stability of Pseudo emulsion film stability is an important parameter to take into consideration while determining foam's stability (Telmadarreie and Trivedi 2018; Vikingstad et al. 2005).

The stabilizing effect of oil depends on its nature. If the oil is solubilized or emulsified and accumulated in the plateau border, it inhibits the liquid drainage due to increased hydrodynamic resistance (Koczo et al. 1992).

Another factor known as Lamella rupture frequency (f_b) is introduced for oil contaminated foams by (Schramm and Novosad 1992):

$$f_b(s^{-1}) = 0.021 * \log L + 0.012 \quad (2.25)$$

This equation gives a good correlation between foam stability and lamella number (L). The addition of foaming agents like polymers enhance the stability of foam in presence of oil (Telmadarreie and Trivedi 2018; Govindu 2020). Also, smaller alkanes destabilize foam whereas larger alkanes stabilize it (Vikingstad et al. 2005). An overview of effect of oil in aqueous foam with regards to oil-foam interaction is shown in (Fig. 2.12).

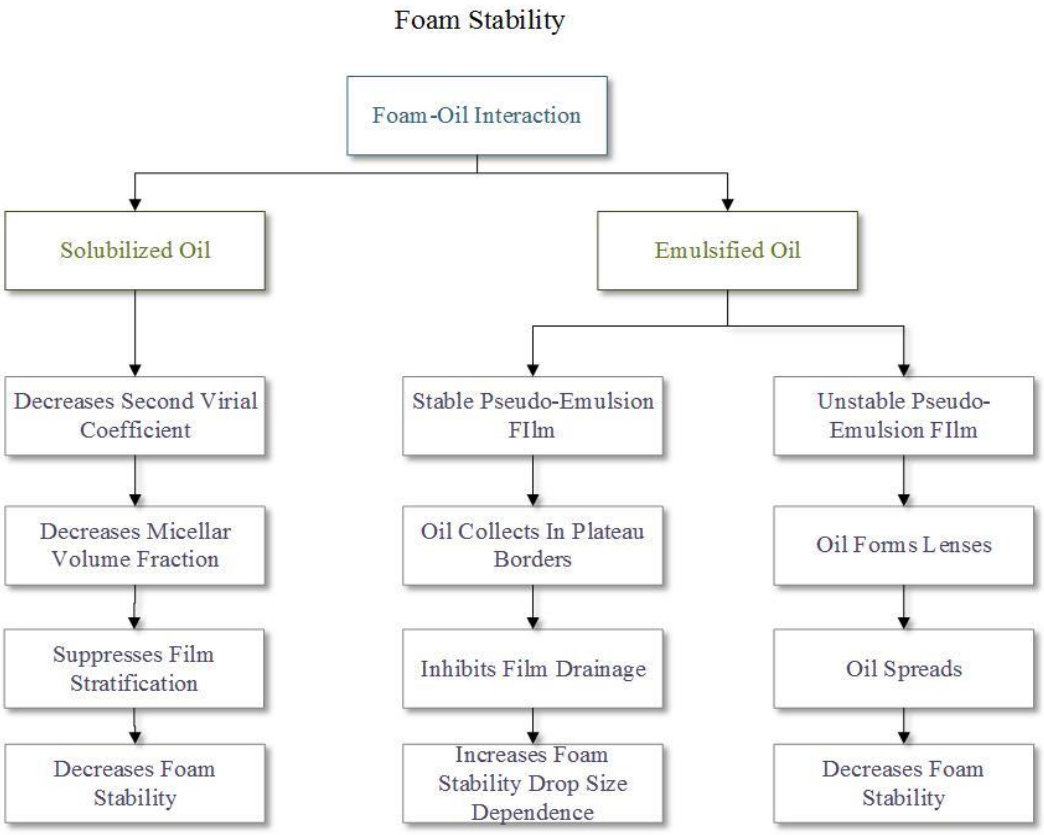

Figure 2.12: Foam stability classification in presence of oil (Reproduced from Koczo et al. 1991)

3. CHAPTER THREE

In this investigation, aqueous foams were tested to study the influence of pressure, foam quality, oil contaminant on foam drainage and bubble size distribution at ambient temperature. The tests were conducted with maintaining the same procedure and environmental conditions to avoid any inconsistency in measurements and minimize the error. This chapter presents in detail the experimental setup, test material, and their properties, test procedure, scope of the experiment, data acquisition and analysis.

3.1 Experimental Setup

The experimental setup used for this investigation is a foam circulating flow loop (Fig. 3.1) consists mainly of two sections: (a) Drainage test section and (b) Rheology test section. A 1000 mL base liquid tank (liquid reservoir) was used for introducing base liquid containing a mixture of water, surfactant, and oil as needed. The mixture was introduced into the system by opening a valve installed below the tank. The entire system was filled with the surfactant mixture with the help of a gear pump powered by a motor with variable frequency drive (VFD) control (Fig. 3.2). Nitrogen was introduced in the foam generation section and mixed with the surfactant mixture. This mixture was foamed with help of a needle valve placed between two static mixers. A flow meter was used to monitor the flow rate and density of the generated foam.

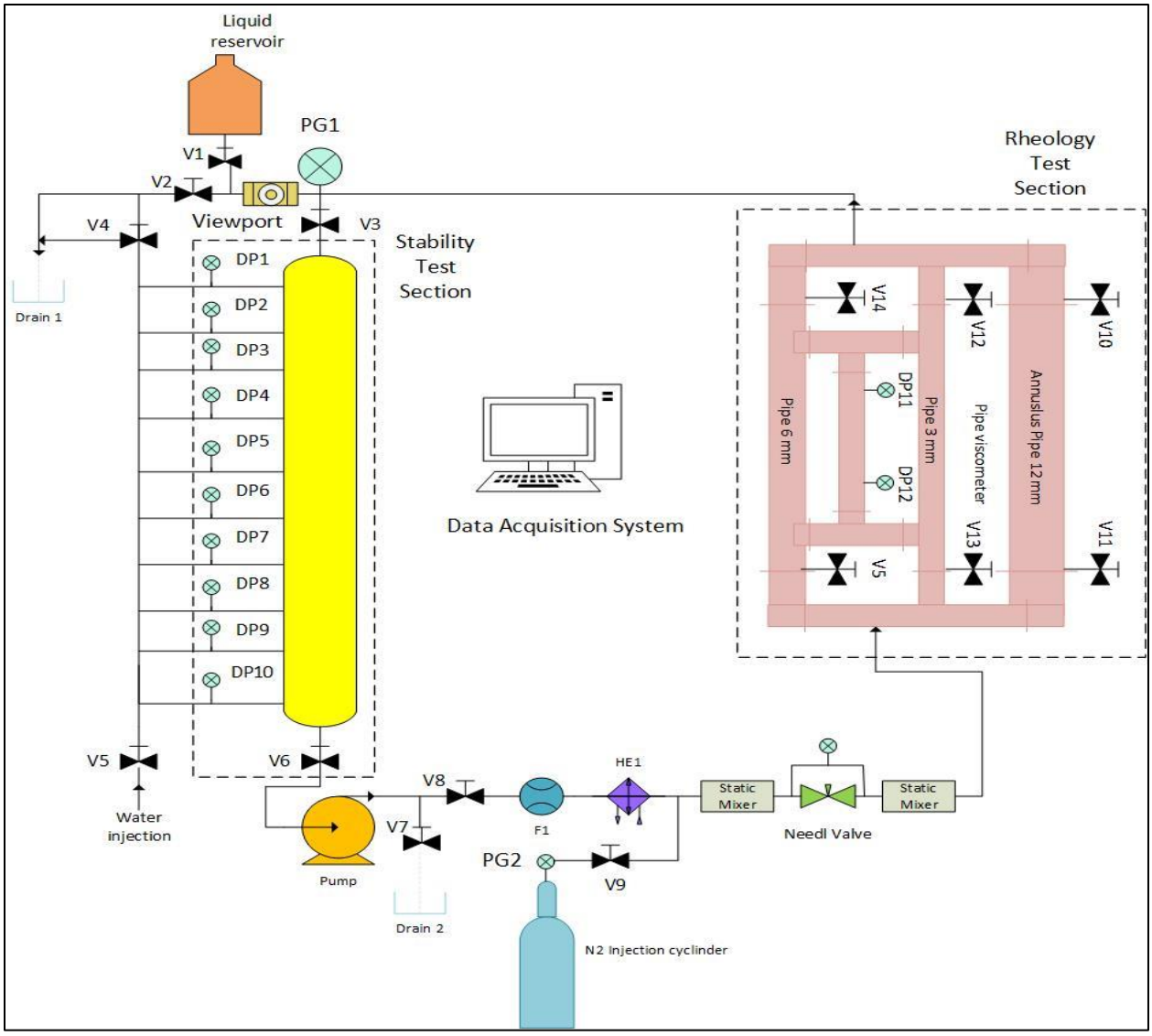

Figure 3.1: Schematic of the experimental setup

The drainage test section contains a vertical column with a height of 1.93 m. The foam was trapped in this section with the help of two automated valves. The foam drainage is calculated by measuring the differential pressure with the help of 10 differential pressure transducers dividing the vertical column into 9 tests segments (Fig. 3.3). The vertical column was pressurized with the help of nitrogen gas and the pressure was controlled by a pressure regulator installed on nitrogen supply cylinder.

Figure 3.2: Motor and Pump

Figure 3.3: Experimental setup of vertical drainage test section

An optical microscopic camera (Dinolite Model AD7013MT) and a viewport were installed at the inlet of the vertical column to capture images of the foam structure (Fig. 3.4). The camera has built-in illumination with the help of 8 white LED's. The scope of the camera ranges from 10x-240x magnification. The camera has calibration features and accurately analyze the bubble size distribution in the image with the help of a software provided with the camera.

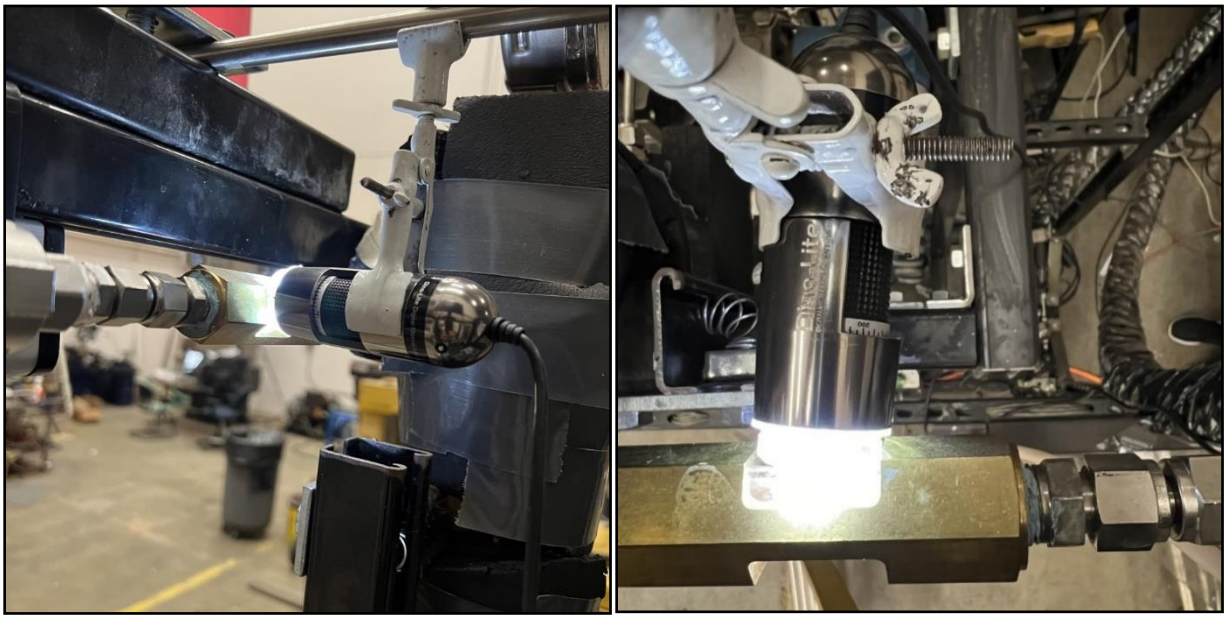

Figure 3.4: Optical microscope with viewport at the side angle (left) and top angle (right)

3.2 Test Materials

Aqueous foams of varying qualities (40%, 50 %, and 60%) were generated in the above-mentioned experimental setup using water, surfactant, and nitrogen gas. To study the effect of oil contaminant, Drakeol light mineral oil was added to the base liquid (water + surfactant). Tap water (from Norman, Oklahoma) was used in the base liquid mixture.

3.2.1 Surfactant

Aqueous foam was generated using anionic surfactant commonly known as Howco Suds^{TM} (Fig. 3.5). Surfactant was used at 2% concentration which is higher than the CMC value of the

surfactant as indicated in previous studies (Akhtar et al. 2018; Govindu 2019). The surfactant properties are given in Table.3.1:

Table 3.1: Properties of the surfactant used

Howco Suds™	
Physical State	Liquid
Color	Light Yellow
Boiling Point	>300°F
pH range	6.5 – 7.5

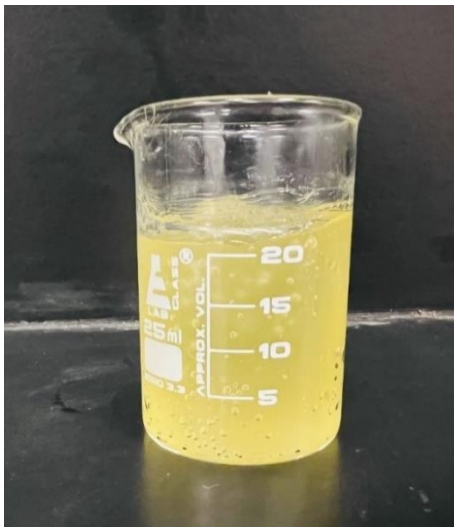

Figure 3.5: Anionic surfactant used for foaming

3.2.2 Oil

Light mineral oil (Fig. 3.6) was used to study the effects of oil contamination on the drainage and structure of foam. Concentration of mineral oil was in range of 0% to 20% by volume with an increment of 10%. White mineral oil is insoluble in hot and cold water. The properties of the oil are given in Table.3.2:

Table 3.2: Properties of Mineral oil

Mineral Oil	
Color	Colorless
Physical state	Liquid
Viscosity (cP)	38.4
Density (g/cm^3)	0.82
API gravity	35

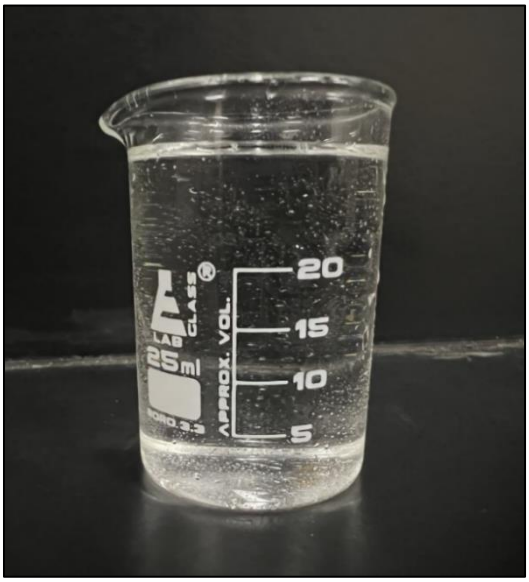

Figure 3.6: Drakeol Mineral Oil

3.2.3 Nitrogen Gas

Technical grade nitrogen gas (99.9%) was used as a gaseous phase for generating foam. The gas was supplied in a high-pressure (20 MPa) cylinder (Fig. 3.7). The gas was injected into the flow loop to control foam quality and system pressurize. Using nitrogen foams has several benefits due to its properties like:

a) Inertness

b) Non-flammability

c) Low solubility

d) Low environmental impact.

Figure 3.7: Compressed nitrogen cylinder with pressure gauge

3.3 Test Procedure

This section describes the experimental procedure used to generate foam in the flow loop. Controlling the pressure in the system and achieving foam of desired quality are two major operations in this process.

For the base liquid preparation, a mixture of water and surfactant is created. The surfactant concentration used was 2% v/v of water. So, for 2 L of water used, 40 mL of surfactant was added and mixed for 10 minutes with a laboratory stirrer for homogeneity (Fig. 3.8). Two drops of pink dye were added to improve the visibility of bubbles while capturing images. To study the effects of presence of oil contaminant at different concentrations, oil was added to the water-surfactant mixture and stirred for 10 minutes for dispersing mineral oil in water.

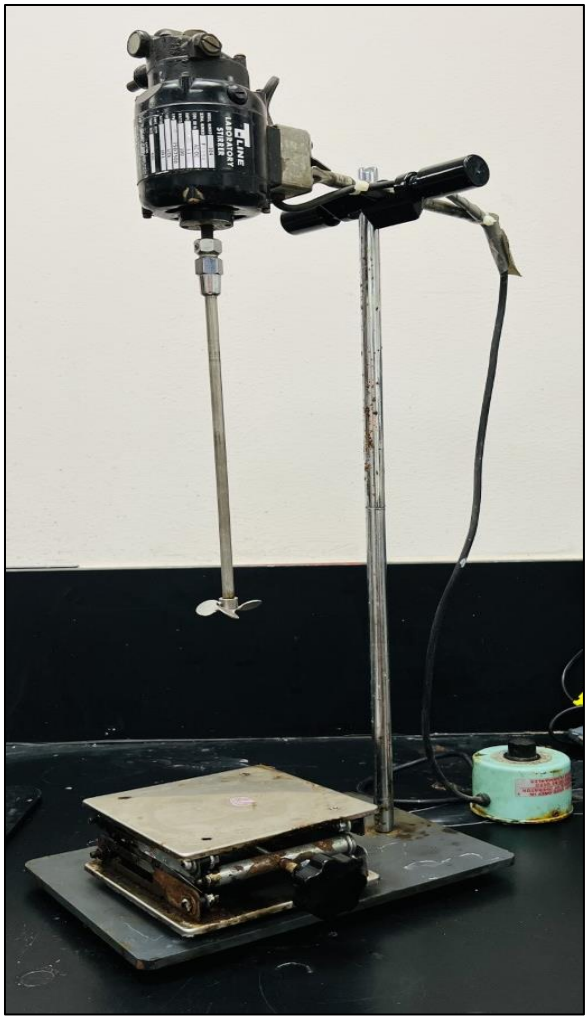

Figure 3.8: Laboratory stirrer controlled with a rheostat

Once the base liquid was ready, it was filled in the 1-L liquid tank (Fig. 3.9), and valve V1 was opened to fill up the entire flow loop. The reverse flow of the base liquid was prevented with the help of a check valve. The valve V2 is kept completely open to release back pressure from the system and allow the free flow of base liquid into the flow loop. After the system was filled with base liquid, both valves (V1 and V2) were closed, and the motor was started at full capacity. The base liquid was pumped through the entire system keeping all pipe viscometers open to allow maximum flow area for the fluid. Nitrogen gas was introduced into the system at the desired pressure, and the needle valve was kept open to allow circulation while mixing the gas and the liquid phases.

Figure 3.9: Liquid tank filled with base liquid

Then the needle valve was throttled to generate foam. For all experiments, a differential pressure of 500 inches of water between upstream and downstream of the valve was maintained to ensure uniform foam generation (Akhtar 2017; Akhtar et al. 2018; Obisesan et al. 2020). As the base liquid turned into a foam of constant quality, it was compared to the desired quality of foam. If the desired foam quality was not achieved, the liquid phase was slowly drained through Valve V7 while injecting nitrogen to maintain pressure. And the system was closed again to regenerate the foam and measure its quality. This step-by-step procedure was repeated until the desired quality of foam was achieved. The foam was circulated for an additional 5 minutes after the desired quality was achieved to make sure the foam has been fully generated and is stable while flowing.

For the stability test, the foam was trapped in the vertical section to allow drainage of the liquid phase. During this test, the motor was shut off, and valves V3 and V6 were closed to trap

the foam. The pressure distribution in the column was measured using differential pressure transducers for two hours. The images of the trapped foam were captured at 30, 60, 90, and 120 minutes of the stability test from the viewport (Fig. 3.10).

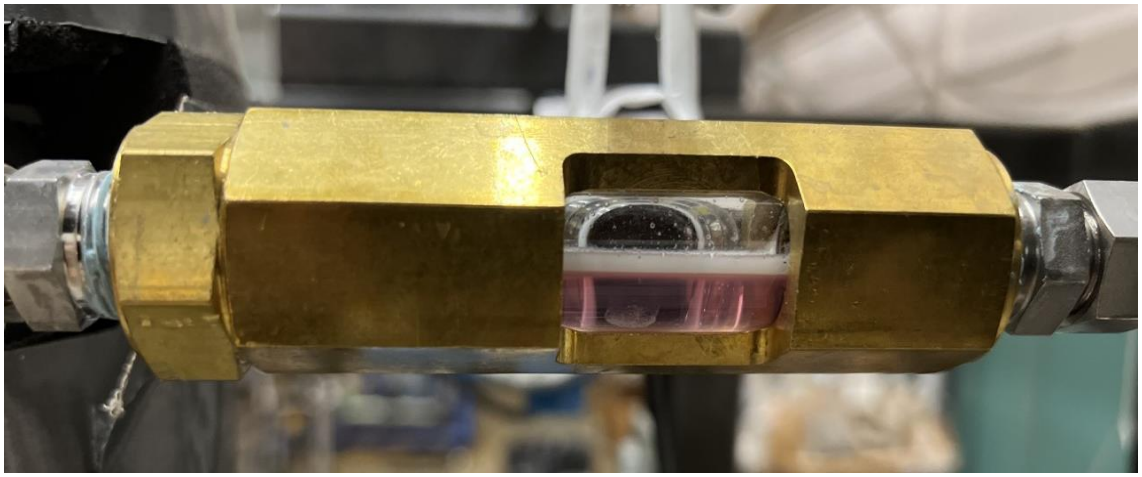

Figure 3.10: Visual cell with base fluid

A commercial software (DinoCapture) supplied with the camera was used to capture images using the digital microscope. All the data collected from the stability test is analyzed and drainage of foam is calculated as a measure for foam stability. Bubble size distribution is obtained by digital image processing using DinoCapture and ImageJ software.

3.4 Experimental Scope

In this study, we tested aqueous foams to see the influence of pressure, foam quality, and oil contaminant on drainage and bubble size distribution. The pressure rating on the viewport (425 psi) is the limiting factor for the test pressure. The data from the stability test is acquired using VBA in Excel from the sensors connected to the data acquisition board. The pressure variations along the vertical column are the important measurements to determine the drainage of the foam over two hours and observe the effect of test parameters on the half-life of the foams. While generating foam, data collected to ensure good quality foams include flowrate, density,

temperature, system pressure, and pressure differential across the needle valve pressure. Foam densities are normalized with the initial foam densities of each section. Normalized foam density chart (Fig. 3.11) gives us information about the changing densities of trapped foam in each segment of the vertical column. As the drainage test starts, the liquid starts draining from the top sections which is monitored by pressure sensors. As a result of the drainage, lower sections start gaining liquid and their densities start increasing and later the curve flattens which means that the lower segments are filled with liquid.

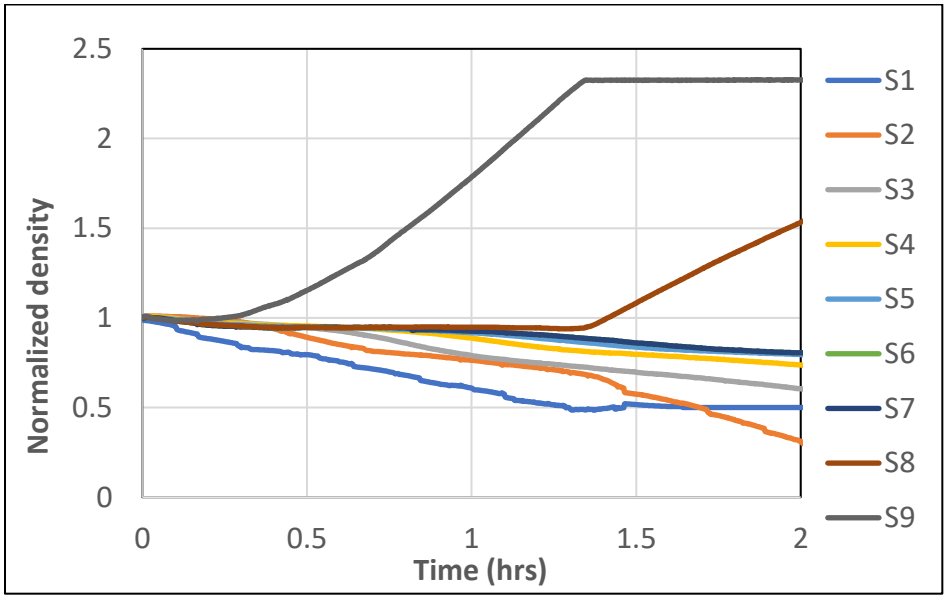

Figure 3.11: Normalized foam column density for each section for the period of drainage test for 60% quality foam.

While generating foam, flowrate data has been captured from starting with base liquid till the achieving the desired foam quality. From Fig. 3.12, we can see that initially the density measurements were unstable. But as the foam is fully generated, we get homogenous foam with constant density.

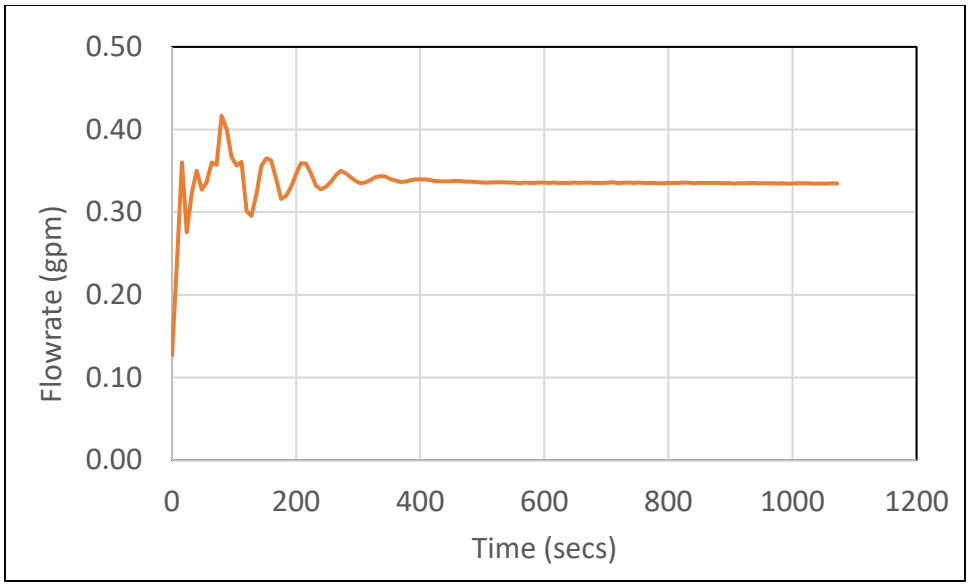

Figure 3.12: Flowrate while generating foam

The test matrix is discussed in Table.3.3:

Table 3.3: Test Matrix

Foam type	Aqueous Foam
Liquid phase	Tap water
Surfactant used (v/v)	Howco Suds^{TM} at 2% concentration
Gas phase	Nitrogen
Dye used	Pink dye (does not change consistency)
Contaminant used	White mineral oil
Contaminant concentration (v/v)	0%, 10%, and 20%
Foam qualities	40%, 50 %, and 60%
System pressure (psi)	100, 250, and 400

A total of 27 tests were performed with each varying combination of pressure, foam quality, and oil concentration. The pink dye was used to give the generated foam a bright color to increase the

quality of taken images and make the bubbles more visible. The foam stability was tested at ambient temperature for all 27 tests.

3.5 Data Analysis

3.5.1 Analysis of Pressure Profiles

For data analysis, the differential pressure is measured across the vertical test section where the foam is trapped. Ten pressure transducers (with an accuracy of ± 5%) divide the vertical column into nine segments (Fig. 3.3). For instance, the segment between DP1 and DP2 is referred as Segment 1, the segment between DP2 and DP3 is named as Segment 2 and so on till Segment 9. The pressure profile measurement helps us to verify the homogeneity of the generated foam in the vertical column. When the pressure profile is linear, the foam in the column is considered as homogenous (Fig. 3.13), and as the liquid film starts draining from the foam structure, the pressure profile becomes non-linear with time.

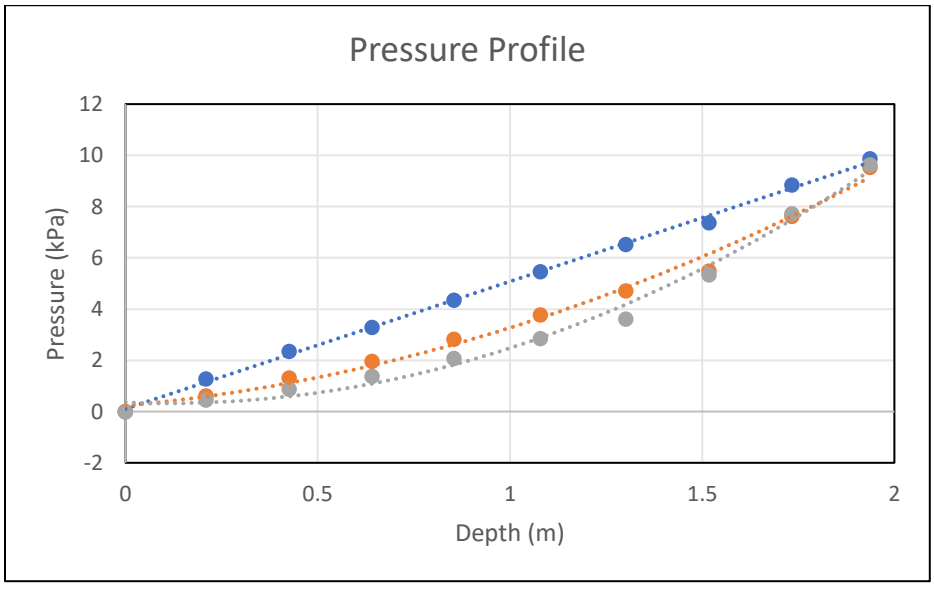

Figure 3.13: Differential pressure profile for generated homogeneous foam

The pressure data obtained from the pressure sensors has units (in. H_20), so it is converted into Kilopascal (kPa). The foam drainage from each segment is determined by applying the pressure profile plots non-linear regression analysis using the second-degree polynomial (Eqn. 3.1).

$$y = C2 * x^2 + (C1 * x) + b \quad (3.1)$$

Where, C1 and C2 are constants and are calculated using excel functions:

C2 = INDEX(LINEST(y, x^{1,2}),1)
C1 = INDEX(LINEST(y, x^{1,2}),1,2)
b = INDEX(LINEST(y, x^{1,2}),1,3)

The known pressure data is fitted as 'x' and the column height is fitted for 'y'. LINEST function is used to calculate the statistics for a straight line that best fits the data and returns an array of constants corresponding to each x-value till we reach constant value 'b'. A LINEST function that is built inside an INDEX function gives specific values that are called in the function as outputs. For our purpose, we can rewrite (Eqn 3.1) as:

$$P = C2 * H^2 + (C1 * H) + b \quad (3.2)$$

On differentiating Eqn. 3.2 with 'H' we get:

$$\frac{dP}{dH} = 2 * C2 * H + C1 \quad (3.3)$$

Where P = pressure data from sensors, H = height of the foam column.

P can be written as hydrostatic pressure head:

$$dP = \rho * g * dH \quad (3.4)$$

Substituting Eqn. 3.4 in eqn. 3.3, we get:

$$\rho * g = 2 * C2 * H + C1 \tag{3.4}$$

$$\rho = \frac{1}{g}(2 * C2 * H + C1) \tag{3.5}$$

Eqn. 3.5 can be used to calculate the density of foam at any height in the vertical test section.

For calculating the average foam density between two segments by substituting 'H' as average height by substituting H=(h1+h2)/2, Eqn.3.5 can be modified as:

$$\rho_{avg} = \left(\frac{1}{g}\right) * [C2 * (h1 + h2) + C1] \tag{3.6}$$

where h1 = Starting height of the foam column segment and h2 = Ending height of the column segment for the vertical foam column.

With the help of these constants (C1 and C2), average density (ρ_{avg}) of the trapped foam is calculated for each segment where there is no liquid loading observed. Only the top 3 segments are considered in the regression analysis because the bottom segments can gain liquid from the drainage of upper segments and consequently exhibit pressure profiles that are different from those of the upper foam-containing segments.

After this, the quality of foam is calculated with the following:

ρ_{avg} = Average Density, ρ_{liq} = Liquid density, ρ_{gas} = Gas density

$$Foam\ Quality = \frac{\left(\frac{1-\rho_{avg}}{\rho_{liq}}\right)}{\left(\frac{1-\rho_{gas}}{\rho_{liq}}\right)} \tag{3.7}$$

The liquid volume (V_{liq})is calculated using the foam quality and the volume of the foam segment ($V_{segment}$) in the vertical column:

$$V_{liq} = (1 - Foam\ quality) * V_{segment} \quad (3.8)$$

As the liquid drains from the foam structure, the volume of gas in the foam increases. The drained liquid is given by:

$$V_{drained}(t) = (1 - Foam\ quality(t)) * V_{liq} \quad (3.9)$$

$$Drainage(t) = V_{drained}(initial) - V_{drained}(t) \quad (3.10)$$

And total drained volume is calculated by:

Where i is the time at which the drainage was calculated. For our experiments, the time duration for the drainage tests lasted up to a minimum of 2 hours.

Final drainage volume is given by:

$$Drainage\ \% = \frac{Drainage(t)}{Drainage(initial)} * 100 \quad (3.11)$$

3.5.2 Foam Image Analysis

Raw images taken from the optical microscope are calibrated for their magnification to provide the correct scale for the respective picture (Fig. 3.14). Magnification was kept constant for all 27 tests to maintain consistency. The raw image is then analyzed using the ImageJ software, where the brightness and threshold of the image were adjusted for the best possible image quality. Once the bubble boundaries are seen clearly, the scale is set for the image, and bubble size is measured for each bubble. A maximum of 100 bubbles are included in the bubble size analysis to give an accurate size distribution at 30, 60, 90, and 120 minutes for each test. The data obtained from these images were related to the drainage data obtained from the stability test to check for any correlation between them.

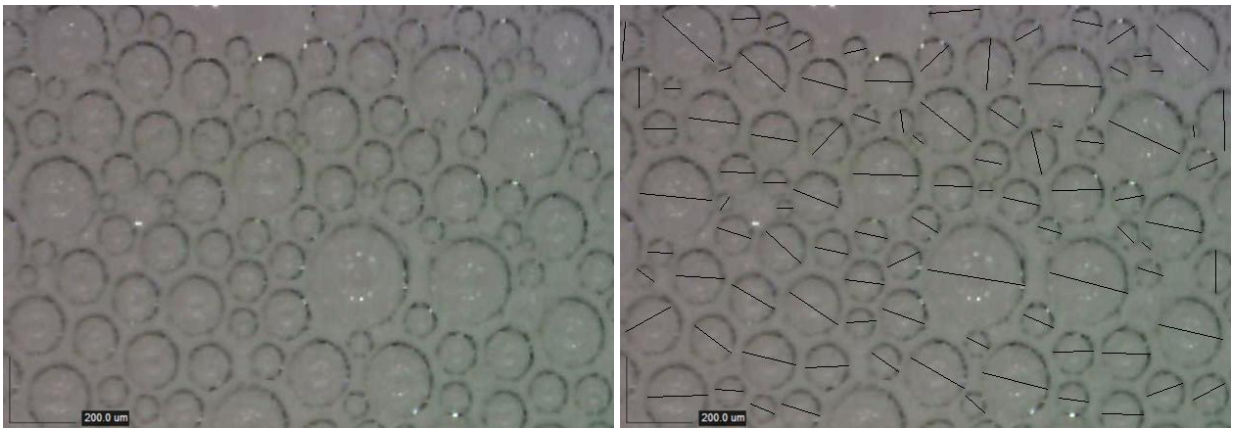

(a) **(b)**

Figure 3.14: (a) Raw image taken from the digital microscope (left) and (b) Image analyzed in ImageJ (Right)

4. CHAPTER FOUR

RESULTS AND DISCUSSIONS

In this section, experimental results are discussed discuss. Drainage measurements are analyzed to understand the stability of aqueous foams and the effects of pressure, quality, and oil contaminant concentration on foam drainage. The bubble structure of foam was examined in each test at an interval of 30 minutes for 2 hours. The examination was performed to understand the relationship between the foam drainage and the bubble size. The test setup, experimental procedure and test conditions were kept constant to minimize experimental error. The homogeneity of foam was maintained while varying foam quality for each test by constantly monitoring the density and flow rate of the foam along with the differential pressure measurements obtained from the pressure transducers along the vertical test section.

4.1 Stability Test

Multiple stability tests were performed to check the repeatability of the drainage tests. From (Fig. 4.1), results for drainage tests for 40% foams at a system pressure of 250 psi are compared.

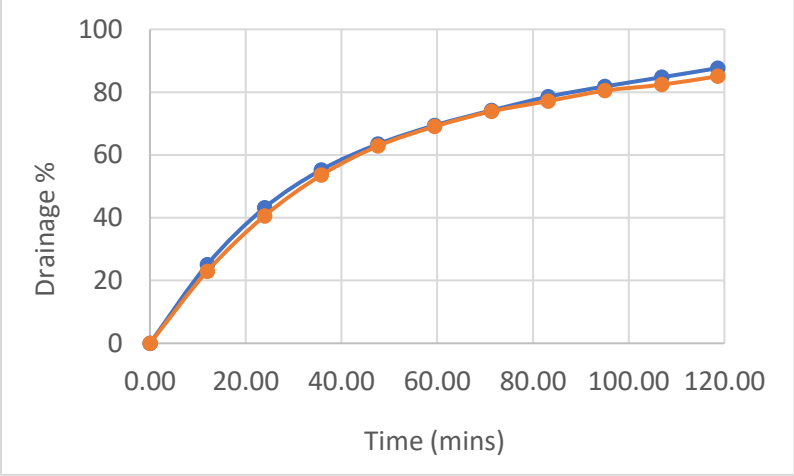

Figure 4.1: Repeatability of drainage tests for foam quality of 40% at system pressure of 250 psi

It is seen that the tests give same results under similar conditions and the error percentage between the drainage measurements of the tests at any given time of the drainage test is less than $\pm$ 2.5 %. Similarly, tests were conducted for different quality of foams for varying conditions and same results within the error percentage would be obtained repeatedly.

As the liquid phase drains from the foam structure, the foam quality increases continuously throughout the 2-hour period of the drainage test. For foam of 40 % quality, not much change is seen in the foam quality profile with increase in pressure (Fig. 4.2a). But for 50% quality foams, with the increase in pressure a decline is observed in the foam quality profile (Fig. 4.2b).

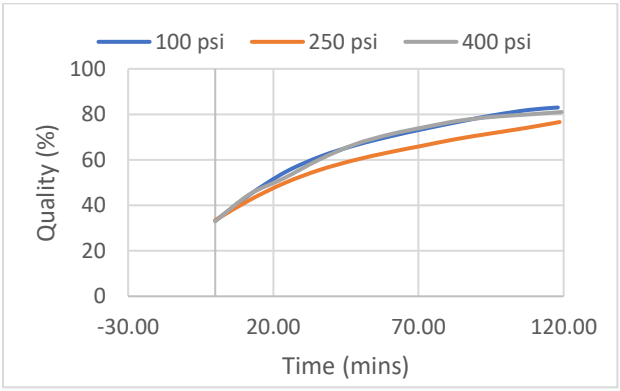

(a)

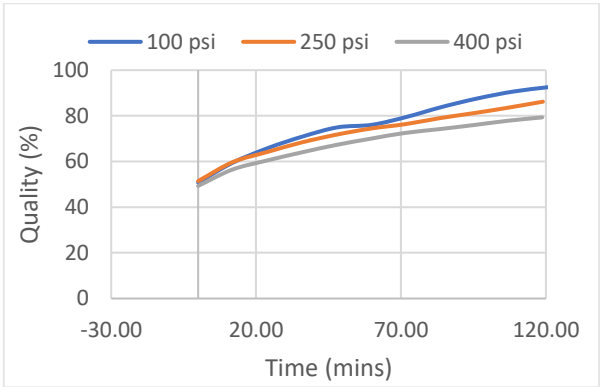

(b)

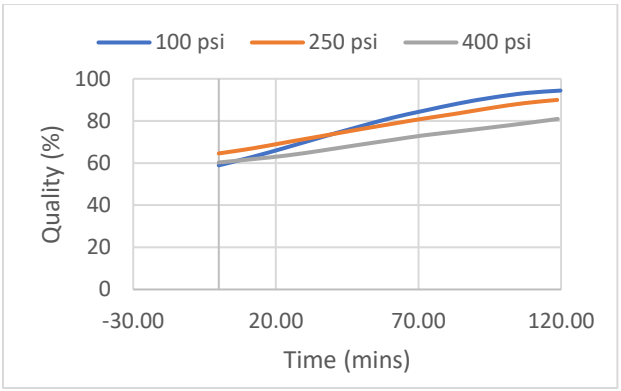

(c)

Figure 4.2: Foam quality profile for the drainage test for pure aqueous foams of different foam qualities (a) 40%, (b) 50%, and (c) 60%

This observation indicated the increase in stability of 50% foam at higher pressures. Same result is observed for foams of 60% quality (Fig. 4.2c).

By looking at the density profile of pure aqueous foams, it is observed that for stable foams the change is density is lower as compared to unstable foams. Continuous monitoring of density is done for the 2-hour period with the help of pressure sensors which have an error percentage of $\pm$ 0.5%. For 50% and 60% foam qualities, it is observed that with the increase in pressure, the change in density is least (Fig. 4.3). This is due to less amount of liquid drainage from the foam system. The overall foam density decreases with increase in foam quality.

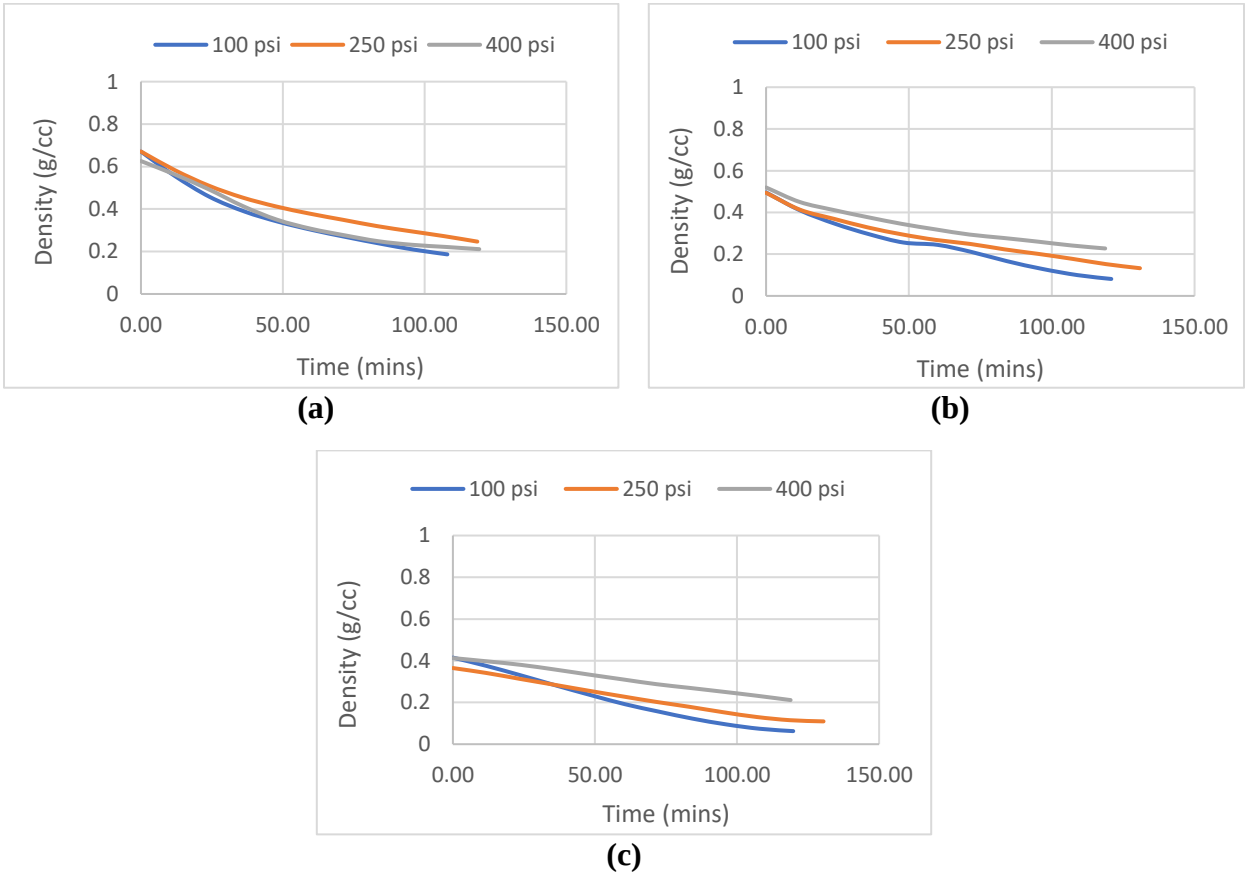

Figure 4.3: Foam density profile for the drainage test for pure aqueous foams of different foam qualities (a) 40%, (b) 50%, and (c) 60%

4.1.1 Aqueous Foam

The initial experiments were conducted with pure aqueous foams (i.e. with no impurities). These tests studied the effects of pressure and quality on aqueous foams' drainage. Drainage of trapped foams in the vertical section is the measurement of foam stability.

First, the effect of varying foam quality can be examined when the system pressure is kept constant (Fig. 4.1). Results show the effect of foam quality on foam drainage at different pressures. At 100 psi (Fig. 4.1a), all foam qualities have approximately 98% drainage at the end of 120 minutes. Although, the foam quality of 60% has a delay of 10 minutes to reach their half-life stage (i.e., drainage of 50%) compared to 40% and 50% foams. This half-life extension implies that the effect of gravitational drainage at low pressure is higher for low-quality foams compared to those of high quality.

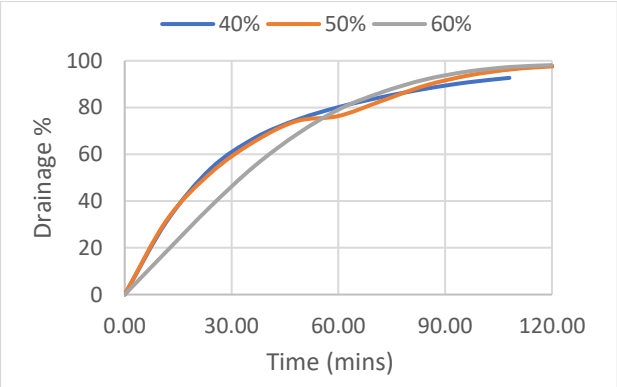

(a)

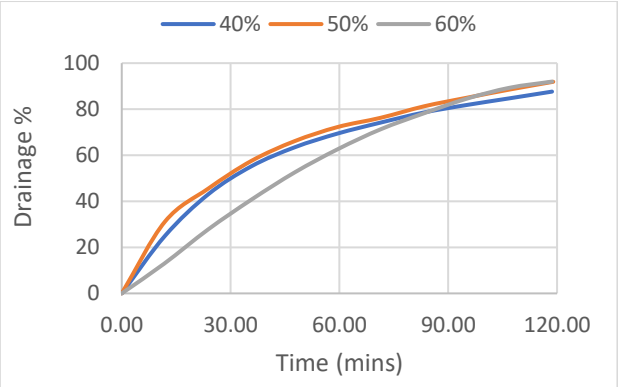

(b)

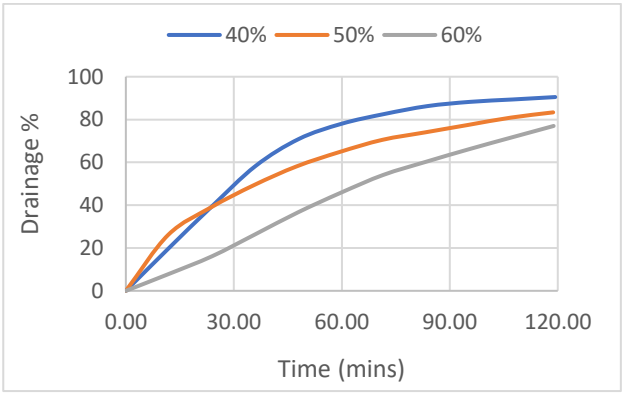

(c)

Figure 4.4: Foam drainage showing the effect of foam quality at different pressures (a) 100 psi, (b) 250 psi, and (c) 400 psi

At later stage, the effects of coalescence and coarsening were similar for all the three qualities. As the system pressure was increased to 250 psi (Fig. 4.1b), the drainage of 60% quality foam increased after 90 minutes compared to those of 40 and 50% quality foams. Overall, the drainage of 40% foam quality was the least (87.6%) at the end of 120 minutes and those of 50 and 60 % quality foams were close to 92%, which are 6% lower than their drainage at system pressure of 100 psi. At 400 psi system pressure, a distinction was observed in the drainage behavior of different quality foams (Fig. 4.1c). The 40% quality foam drained about 90% at the end of 120 minutes and the drainages were lower for 50 and 60% quality foams. The half-life of the foams varied significantly. There was a difference of 35 minutes between 40% and 60% quality foams. This difference demonstrates that increased foam quality at high pressure increases the stability of high-quality foams.

At lower system pressures, low-quality aqueous foams show similar drainage as high-quality foams but have a difference in the half-life time. In other words, high-quality foams are delayed in reaching their half-life time at all pressures, making them more stable than lower quality foams.

The effect of pressure on drainage was investigated at different foam qualities (Fig. 4.2). For 40% quality foams (Fig. 4.2a), the least drainage was observed at system pressure of 250 psi followed by 400 psi. The 40% quality foam was the least stable at a system pressure of 100 psi. The initial drainage rate at 400 psi was low until the foam reached the half-life point and after that, the drainage rate increased considerably until it reached 80% drainage. At 50% and 60% foam qualities, a decrease in the drainage was noticed with system pressure. At higher foam quality of 60% (Fig. 4.2c), there is a clear increase in stability of foams. At foam qualities lower than 50%, a clear pattern with the change in system pressure was not observed. However, at higher foam qualities, increase in pressure extends the half-life of the foam. Thus, it can be said that increase in pressure compresses the gas molecules present in the bubbles which stops the expansion of gas bubbles in the foam structure and gives foam much needed stability.

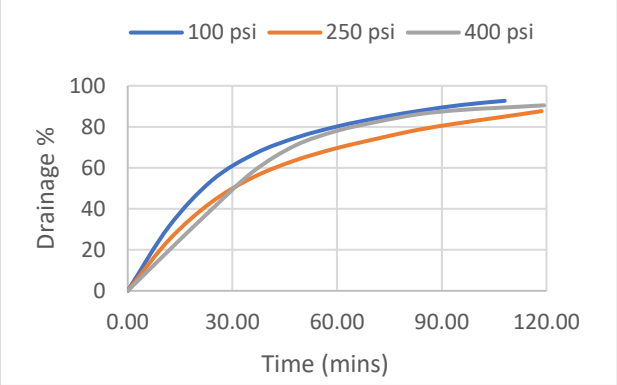

(a)

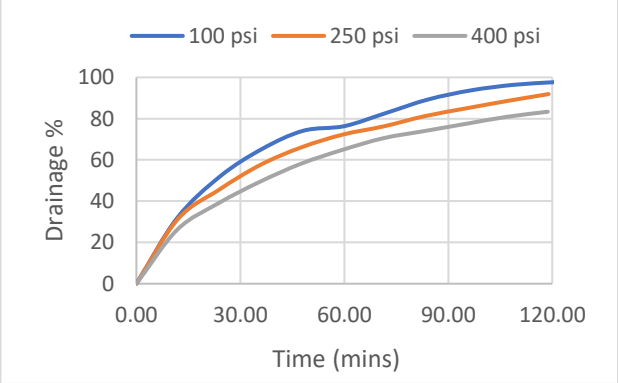

(b)

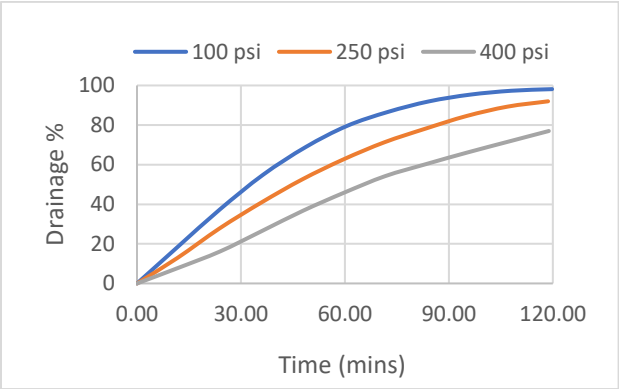

(c)

Figure 4.5: Foam drainage showing the effect of pressure at different foam qualities (a) 40%, (b) 50%, and (c) 60%

4.1.2 Aqueous Foam with 10% Oil

To simulate downhole foam contamination with oil, light mineral oil at 10% concentration v/v was added to the base liquid. The presence of oil could create a layer film of water-oil emulsion around the bubbles. And the stability of this pseudo emulsion film determines the stability of the foam. The effect of pressure on the drainage of contaminated foam was studied at different qualities. At 100 psi (Fig. 4.3a), the highest drainage was observed with 60% quality foam which was close to the drainage of 40% quality foam. 50% quality foam had the least drainage. Although the 60% quality foam was the least stable at the 120-minute mark but had the best half-life time amongst the other foams of lower qualities.

At the intermediate pressure (250 psi), results were similar to the ones observed at 100 psi (Fig. 4.3b) except minor differences. A 6% reduction in the drainages of 40% and 50% quality foams quality were observed while only 2% drainage reduction was recorded for 60% quality foam. The drainage behavior of 60% quality foam have been high throughout these tests. For system pressure of 400 psi, 50% quality foam was most stable showing the lowest drainage of 82.6%.

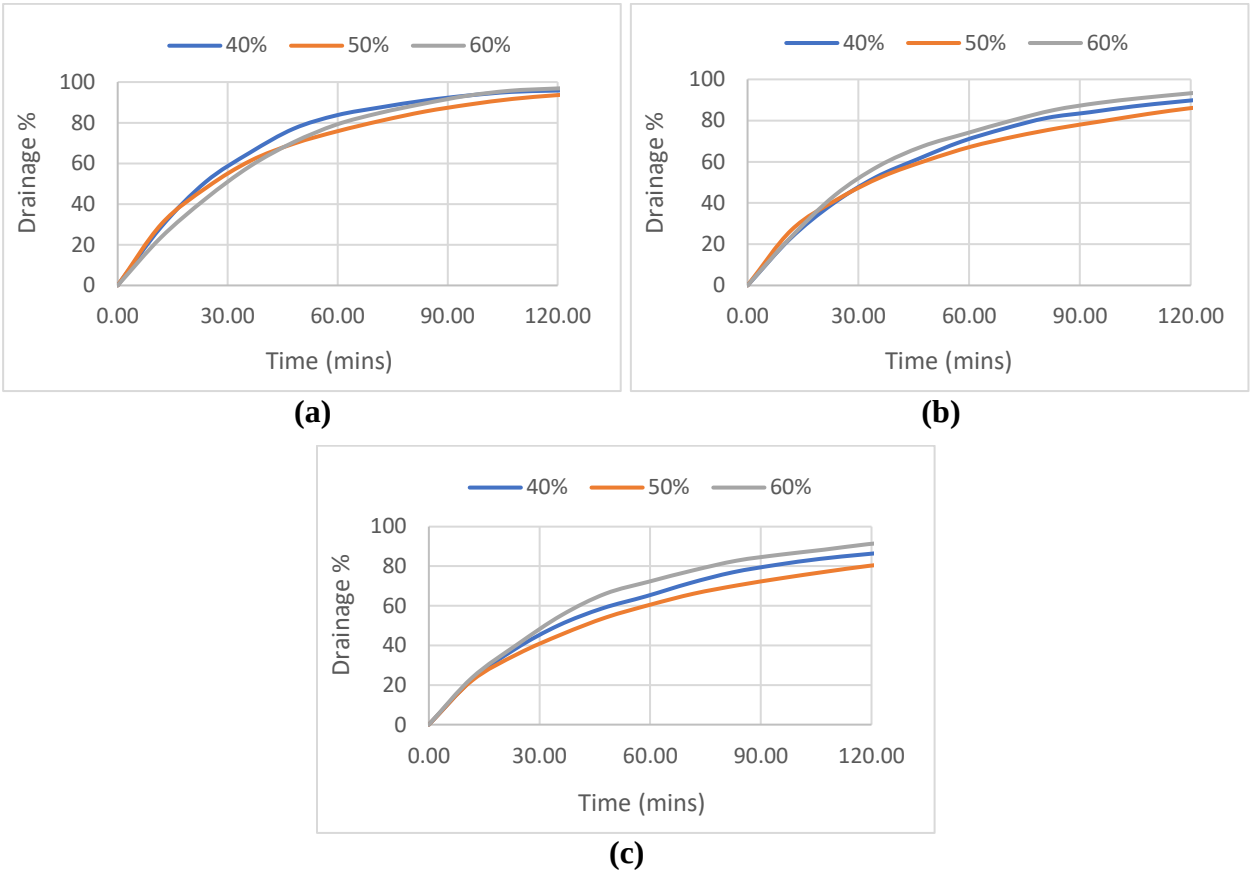

Figure 4.6: Foam drainage showing the effect of foam quality at different pressures (a) 100 psi, (b) 250 psi, and (c) 400 psi (10% oil contamination)

The effect of pressure on the drainage of 10% oil-contaminated foam was studied considering various qualities. For 40% foams (Fig. 4.4a), system pressure of 100 psi gave the least stable foams whereas system pressure of 400 psi had the most stable foams with the final drainage of 88 %. Comparing different quality foams, 50% quality showed slightly better stability regardless of the system pressure (Fig. 4.4b). At 60% foam quality, the effect of pressure on drainage was minimal (Fig. 4.4c).

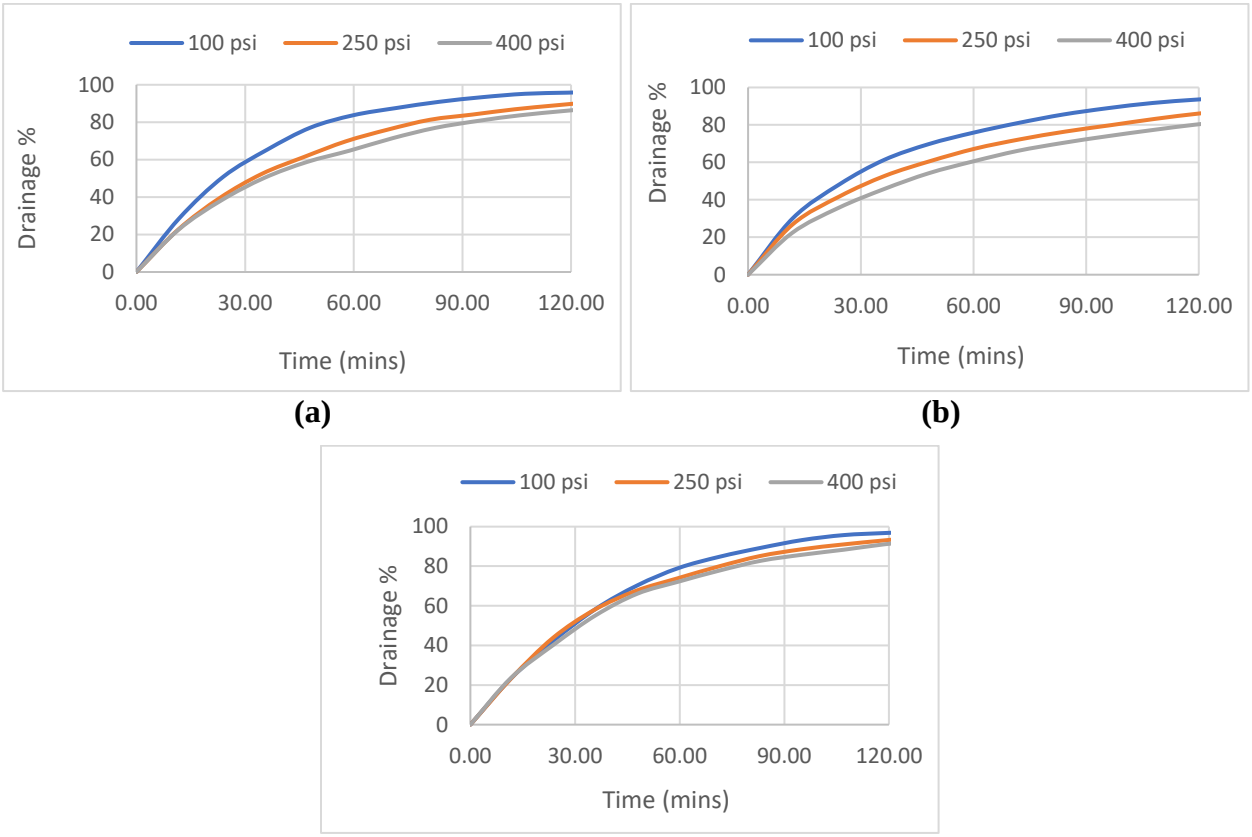

Figure 4.7: Foam drainage showing the effect of pressure at different foam qualities (a) 40%, (b) 50%, and (c) 60% (10% oil contamination)

Overall, with 10% oil contamination, the increase in pressure reduced drainage and improved foam stability for all qualities tested. The foam drainage curves for all qualities have a similar slope and follow each other through the drainage period.

4.1.3 Aqueous Foam with 20% Oil

For the last 9 tests, the mineral oil concentration was increased from 10 to 20% v/v. The contamination is expected to impact the stability of the foam structure by creating a pseudo emulsion film.

The effect of pressure on the drainage of 20% oil-contaminated foam was investigated varying its quality (Fig. 4.5). For system pressure of 100 psi (Fig. 4.5a), 40% quality foam has the lowest drainage of 93.3 %. A 1% reduction in drainage was observed for 60% quality foam

and 50% quality foam were least stable at 95.3 %. There was no a substantial difference in drainage between the three foams. After increasing the pressure to 250 psi (Fig. 4.5b), 50% quality foam exhibited a slightly better stability. In the early drainage stage, 60% foam has a lower drainage than 40% foam but 60% foams become unstable after 80 minutes and drainage kept increasing till the end of 120 minutes whereas the 40% foam stabilizes itself. The drainage for 40 % and 60% foams are 86% and 88.5% respectively. Similar drainage pattern can be seen when the system pressure has been increased to 400 psi (Fig. 4.5c). Lowest drainage of 75.7 % is observed for the 50% quality foam at 400 psi pressure with 20% mineral oil concentration. This is the most stable foam that is observed over the 27 experiments that have been carried out in this study. For 40 and 60 % quality foams, the half-life of 60% quality foam was better. Still, after 80 minutes the 60% quality foam exhibited higher drainage and the 40% quality foam has stabilized and drainage reduces significantly similar to drainage at 100 psi.

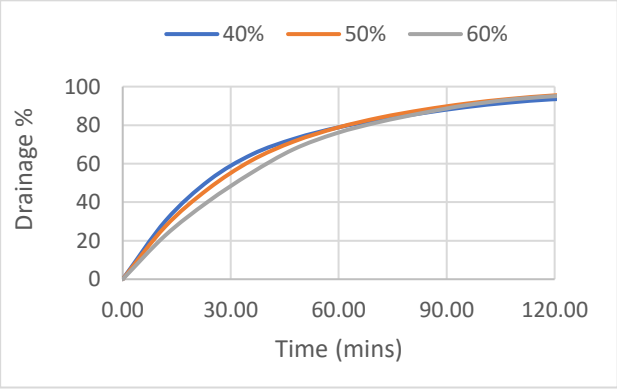

(a)

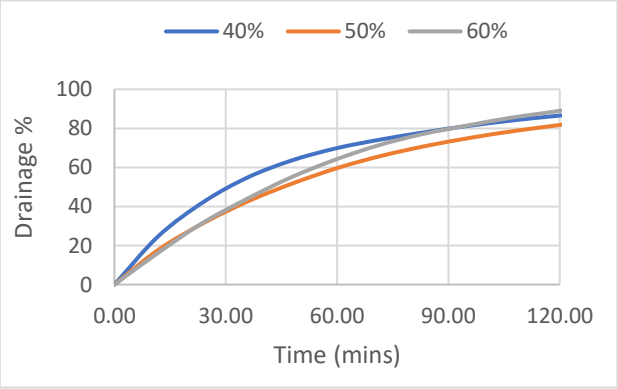

(b)

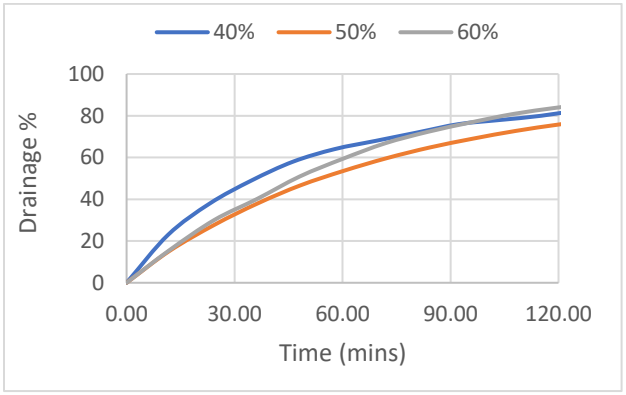

(c)

Figure 4.8: Foam drainage showing the effect of foam quality at different pressures (a) 100 psi, (b) 250 psi, and (c) 400 psi (20% oil contamination)

Results presented in Fig. 4.5 are rearrange for different qualities in Fig. 4.6. For 40% quality foams (Fig. 4.6a), the one generated at 100 psi was the least stable showing the final drainage of 93.3%. Then, its drainage dropped by 9% at 250 psi. Further increase in the pressure to 400 psi reduced the drainage to 80%, which is the lowest for 40% quality foams. Results obtained at 60% foam quality (Fig. 4.6c) are consistent with the ones observed at 40% quality.

For 50% quality foams (Fig. 4.6b), there is noticeable difference in the drainage measured at different pressures. The drainage decreased with pressure indicating a notable increase in stability at 400 psi. The improvement in stability could be attributed to two factors: a) compression of gas molecules in the bubbles restricting the rapid expansion of gas, and b) the stability of pseudo emulsion film resulting from the addition of 20% mineral oil stabilizing the bubbles in foam structure and slow down bubble film rupturing. Overall, the effect of quality study demonstrated that 50% foams were more stable than 40% and 60 % quality foams.

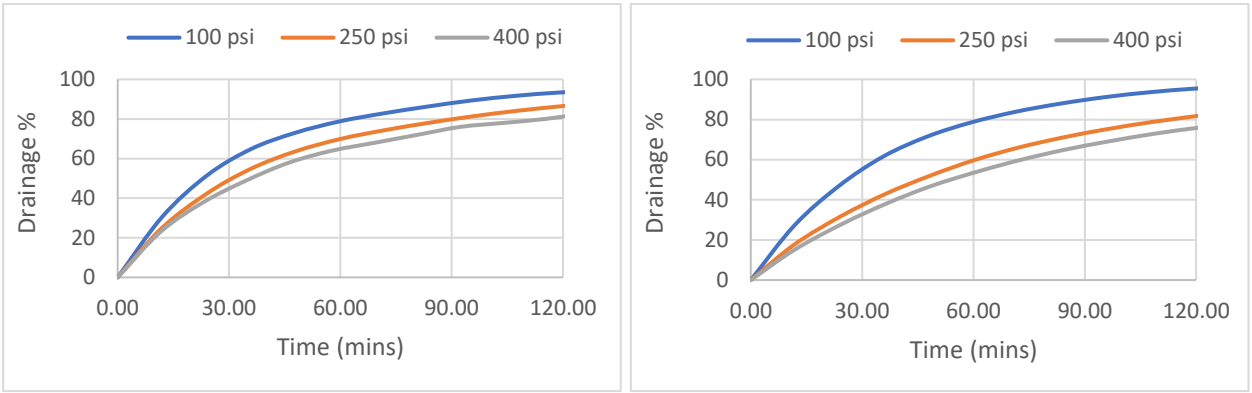

(a) **(b)**

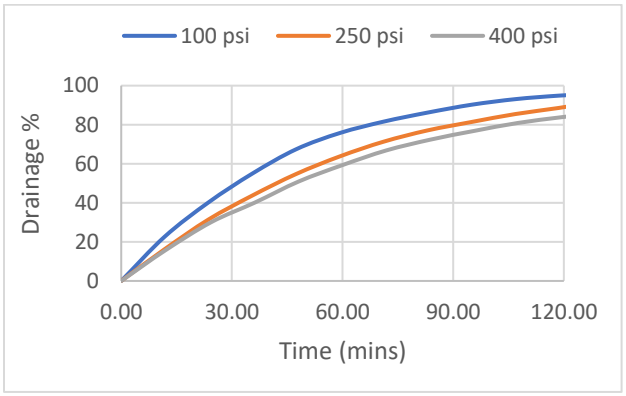

(c)

Figure 4.9: Foam drainage showing the effect of pressure at different foam qualities (a) 40%, (b) 50%, and (c) 60% (20% oil contamination)

4.1.4 Effect of Oil Contamination

The effect of oil concentration on the drainage of 40%, 50% and 60% foam quality are compared in this section. Oil contaminant affects the stability of foam structure due to the formation of pseudo emulsion film formed on the bubble boundary. The comparison is made for the trapped foam at system pressure of 100 and 400 psi (Fig. 4.7). For foams of 40% qualities (Fig. 4.7a), we can see that at 0% oil concentration there is minor improvement in the foam stability at 400 psi as compared to 100 psi. When 10% v/v mineral oil is added, there is a 10% reduction in the drainage rate for 400 psi. Foams at 400 psi, become more stable when 20% v/v oil concentration is added to the base liquid mixture. Addition of oil to 40% foams at 100 psi, did not impact the

stability of the foams majorly whereas the drainage reduced significantly for experiments conducted at 400 psi.

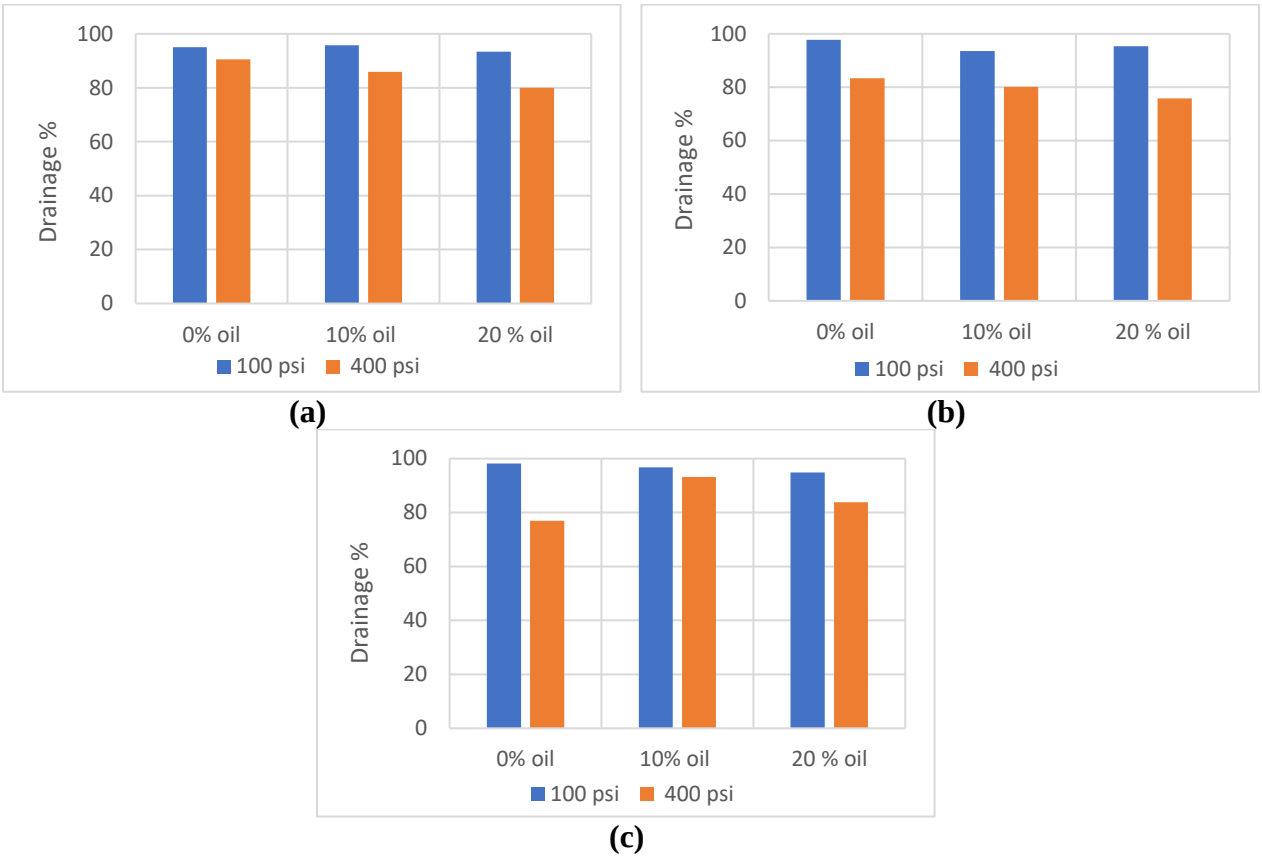

Figure 4.10: Comparison of results of drainage test at 100 psi and 400 psi for foam qualities of (a)40% (b) 50% and (c) 60%

Now, comparing the drainage tests for 50% at 100 psi (Fig. 4.7b), not much difference is seen on addition of mineral oil at different concentrations but at 400 psi the drainage rate reduces with the increase in oil concentration. The reduction in drainage rate at100 psi and 400 psi for 50% foams for pure foams and 10% oil contaminated foams is identical. Addition of 20 % mineral oil, stabilizes the foam structure at 400 psi but impacts negatively to stability at 100 psi. For 60% foam quality at 100 psi (Fig. 4.7c), there is only a slight increase in stability with addition of mineral oil but at 400 psi addition of oil destabilizes the foam structure. For pure aqueous foams of 60% foams, the drainage rate is least for foams at 400 psi without any added

contamination. Overall, the foam structures are more stable at higher pressure and increasing the addition of oil decreases the drainage rate except for pure foams of 60% quality.

4.2 Bubble Size Distribution

The second study was conducted to understand the relationship of bubble size in the foam structure with both the varying effects of quality and pressure. The bubble size distribution is important to establish a relationship between foam drainage and the bubble size distribution. Therefore, different factors that can affect the bubble size are experimentally studied. While the generated foam was trapped in the vertical column and its bubble structure was monitored through a viewport installed at the column's entrance. The images captured from the viewport are analyzed and their average bubble size is noted at interval of 30 minutes. In this section, the results of the bubble size analysis are presented.

4.2.1 Aqueous Foams

The effects of quality and pressure on bubble size are discussed in this section. As anticipated, the average bubble size decreased with pressure and increased with foam quality. However, it is important to note that the impact of quality on bubble size diminished as the pressure increased. Also, the rate of change of bubble size (the slope of bubble size versus time plot) significantly reduced with pressure indicating the reduction of drainage and improvement of foam stability with pressure.

At 100 psi, drainage was the least for 40% foam quality (Fig. 4.1a), and the bubble size was the minimum throughout the test (Fig. 4.8a). At 30 minutes, the average bubble size was 78 µm and increased to 92 µm at 60 minutes, and finally, the average bubble size was 132 µm. For 50% foam, there has been an increase in the overall bubble size when compared to 40% quality bubbles. This increase in bubble size is due to an increase in the volume of gas to achieve the

desired foam quality. The average bubble size for 50% foam was 101 µm at 30 minutes and 168.6 µm at the end of the experiment. Interestingly, for 60% quality foam, the average bubble size was 213 µm at 90 minutes and 125 µm at the beginning of the test. This pattern continued at the end of the test as the average bubble size increased to 268 µm.

As the pressure is increased to 250 psi (4.8b), there is an approximately 30% reduction in the average bubble size of the foams at all three qualities. The average bubble sizes of 60% quality foams at 100 and 250 psi have slightly higher slopes than other foam qualities at the same pressure, which makes the foam less stable at these pressures. This observation is consistent with drainage measurements (Fig. 4.1). As the system pressure was increased to 400 psi, the bubble size did not change significantly with time, demonstrating the improvement in the stability of the foams.

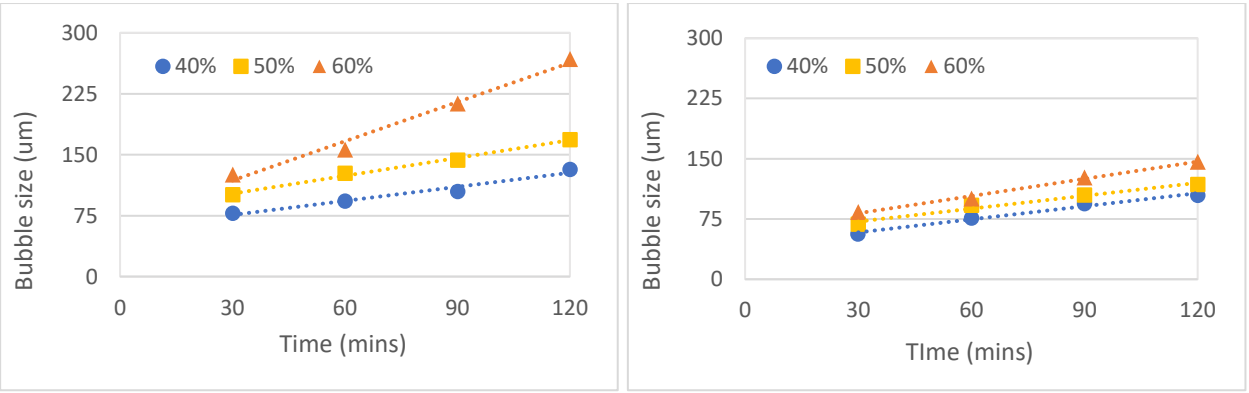

(a) **(b)**

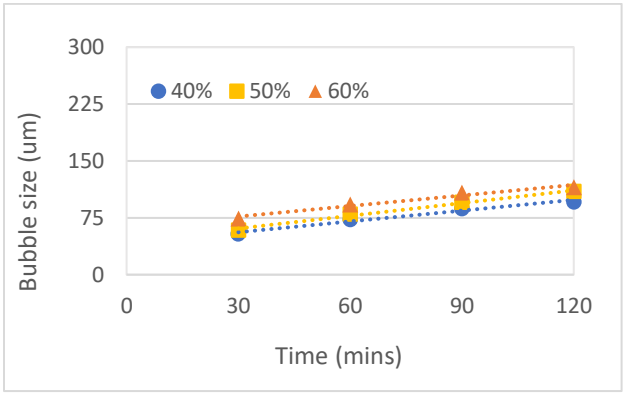

(c)

Figure 4.11: Average bubble size showing the effect of foam quality at different pressures (a) 100 psi, (b) 250 psi, and (c) 400 psi

4.2.2 Aqueous Foams with 10% Oil

When 10 % mineral oil was added, some changes in the average bubble size distribution patterns was observed as compared to pure aqueous foams as discussed in the previous section. The bubble size appears to have slightly shrunk (Figs. 4.8 and 4.9) due to oil particles in the foam structure. The effect of foam quality on bubble size distribution was studied at different (40%, 50% and 60%) foam qualities. Initially, the system pressure was set at 100 psi and there was hardly any change in the average bubble size of 40% quality foam with and without oil contaminant. Foam with 50% quality was very stable as it exhibited a very slow rate of bubble size growth. At 30 mins, the average bubble size was 97.6 µm and it reached 134 µm at 120 minutes. Although 60% foams (Fig. 4.9a), had a higher slope than foams of other qualities, it was more stable than pure aqueous foams at 100 psi. Like the clean aqueous foam, with increasing pressure, the impact of foam quality on drainage diminished as indicated by the overlapping/bundling of average bubble size plots of different quality foams.

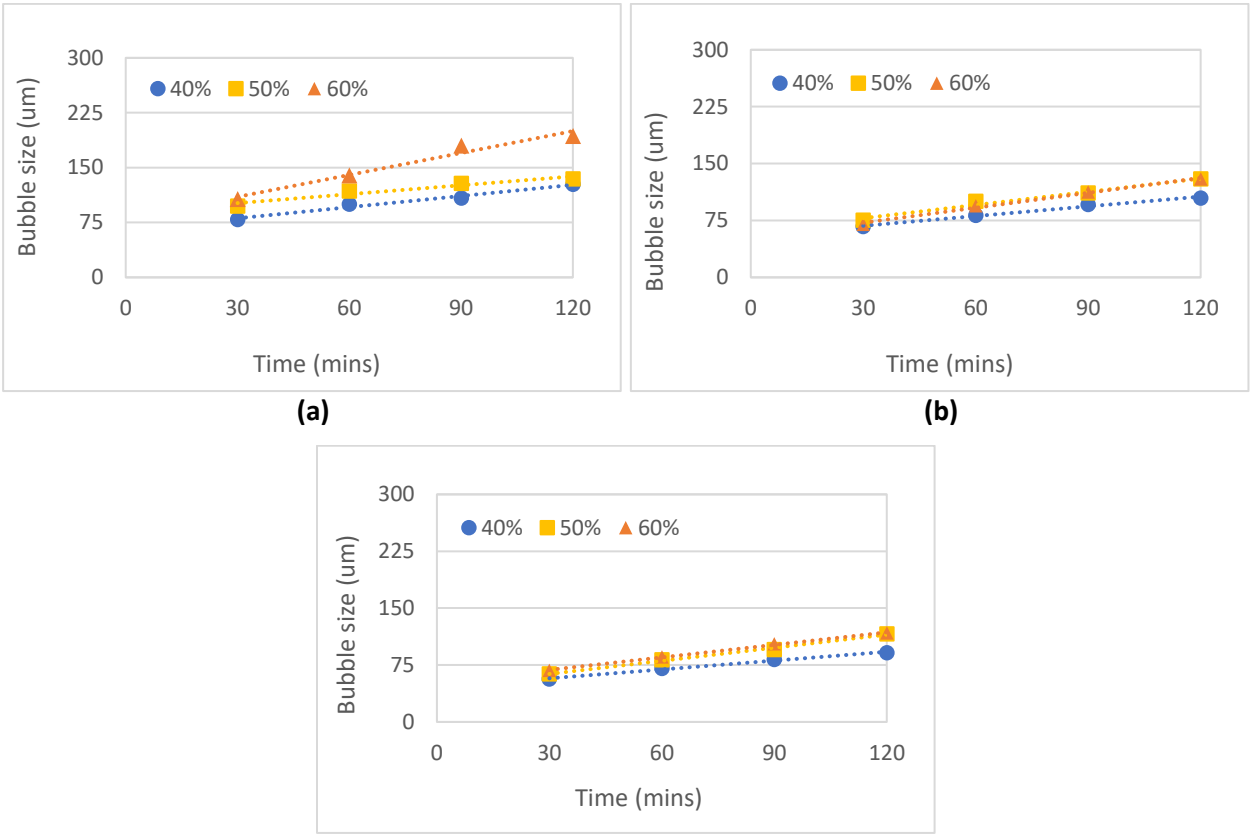

Figure 4.12: Average bubble size showing the effect of foam quality at different pressures (a) 100 psi, (b) 250 psi, and (c) 400 psi (with 10% oil contamination)

4.2.3 Aqueous Foams with 20% Oil

The mineral oil contamination was increased to 20% to study the oil-water interaction in foam structure at elevated oil concentration (Fig. 4.10). With increasing oil concentration, the impact of foam quality on drainage reduced regardless of the pressure. The reduction is indicated by the crowding of the average bubble size plots of different quality foams. Moreover, the impact of pressure on the drainage significantly reduced with the increase in oil concentration. Adding 20% oil contaminant also decreased the average bubble size of the foams, indicating the formation of stable pseudo emulsion films around the bubbles.

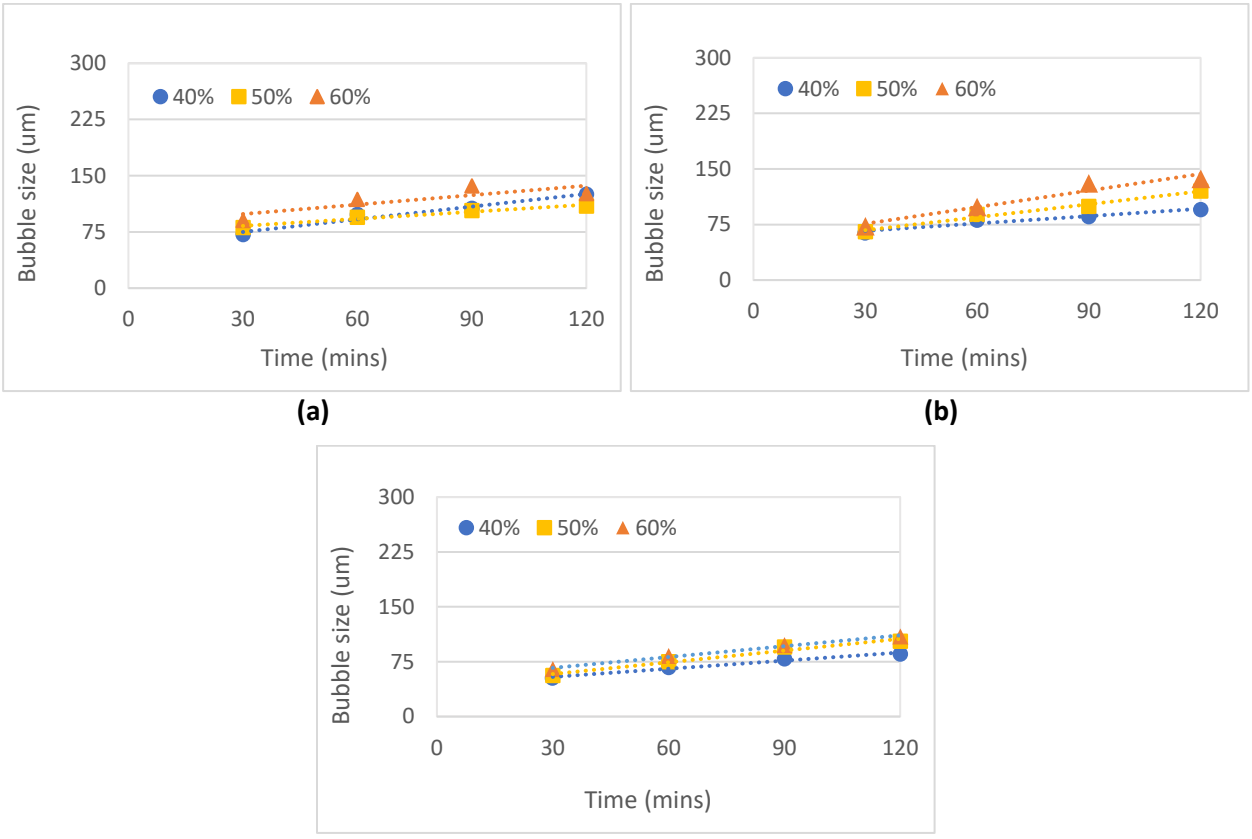

Figure 4.13: Average bubble size showing the effect of foam quality at different pressures (a) 100 psi, (b) 250 psi, and (c) 400 psi (with 20% oil contamination)

5. CHAPTER FIVE

Conclusion and Recommendations

In this study, a total of 27 tests for measuring drainage of liquid phase from the homogenously generated trapped foam column. Each drainage test lasted for 2 hours, and pressure data was collected with a data acquisition system. In addition to that, 108 images (4 images per drainage test) were analyzed to get data for average bubble size distribution. These images were captured with a digital microscope and a method was developed to measure the bubble diameter for each image. This section has been divided into two subsections (a) Conclusions and (b) Recommendations. First, the conclusions for three sets of foam drainage tests based on varying mineral oil contamination will be presented followed by recommendations for further experimentation to improve the understanding of the drainage behavior of foams and impact on bubble size.

5.1 Conclusions

The outcomes of foam stability investigation conducted by varying foam qualities, system pressure, and mineral oil concentration are summarized here. All tests were conducted at ambient temperatures and with the same foam generation technique using a closed flow loop to achieve consistency in the measurements.

- Bubble size in the foam structure varies with foam quality at constant pressure, as foam quality depends on the amount of gas volume present in the foam structure. The higher the foam quality is, the larger the bubble size of the foam structure. Nonetheless, with the addition of contaminant oil, the effect of foam quality on the bubble size reduced noticeably.

- With time, foam bubble size increased, confirming the coarsening and coalescence of foam bubbles. When the foam structure is unstable, the bubble growth rate increases due to the exacerbation of bubble coalescence and coarsening.
- An increase in pressure reduces the average bubble size of foams. However, with the addition of contaminant oil, the impact of pressure on the foam bubble size diminished significantly.
- Increasing the oil concentration, decreases the difference in average bubble size between varying foam qualities at a constant pressure which means that the difference in the initial bubble size and final bubble size for varying foam qualities diminishes with the increase in oil concentrations.

5.2 Recommendations

Based on the outcomes of the current investigation, the following recommendations are made for future studies:

- It would be impactful to study the effect of temperature on the bubble size distribution and drainage of foam.
- The effect of addition of other downhole contaminants like salt, clay at different concentrations can have different impacts on the foam structure, which affects the bubble size distribution.
- Stabilizing agents like polymers, fused nanoparticles, and fiber can be added to the liquid surfactant mixture to understand their effect on the stability of foam under varying pressure conditions. The effect of these stabilizing agents on the bubble size in the foam structure would be interesting to study.

- Since these tests were conducted in a vertical column, similar tests can be conducted in inclined columns to study the effect of inclination on foam drainage.
- Foam quality can be tested between 40-60% at intervals of 5%, and the surfactant concentration can be varied from 1-3% v/v at an interval of 0.5 % to check for any improvement in the stability of the aqueous foams.

Nomenclature

μ = Liquid viscosity

μ_s = Surface shear viscosity

A = Cross sectional area

D_{eff} = Diffusion efficient of gas

$\partial\varepsilon$ = Geometric constant for bubble

E = Entering coefficient

E = Gibb's elastic modulus

$f(\phi)$ = Fraction of bubble area covered by thin films

f_b = Lamella rupture frequency

g = Acceleration due to gravity

G = Pressure gradient driving the flow

h = Film thickness

H = Foam Height

K = Dimensionless permeability constant

k = foamability of foam

K_1 = Dimensionless number

$K_{1/2}$ = Dimensionless number

K_3 = Permeability constant

K_4 = Permeability constant

K_c^0 = Dimensionless permeability

L = Channel length

M = First mobility parameter

m = Nature of viscous dissipation

N = Second mobility parameter

η = Viscosity

N’ = Number of steps

p = Liquid pressure

ϕ = Liquid volume fraction

R = Radius of bubble

r’ = Radius of curvature of channels

R_{avg} = Average bubble Radius

S_0 = Spreading oil coefficient

S_i = Surface area of bubble i

S_{tot} = Surface area of total foam

S_w = Spreading water coefficient

t = time

T_{coars} = Coarsening time

T_{drain} = Drainage time

u_o = Maximum flow speed

V(t) = Volume of liquid at time 't'

V_f = Final volume of liquid at time, t = 0

z = Height of the container

Z =Position of the grid in foam column

α = Liquid fraction exponent

γ = Surface tension

Δt = Time interval

Υ = Surface tension

Υ_F = Foaming aqueous solution surface tension

Υ_{OF} = Foaming aqueous solution/oil interfacial tension

Υ_{og} = Surface tension between oil-gas phase

Υ_{wg} = Surface tension between water-gas phase

Υ_{wo} = Surface tension between water-oil phase

ϵ = Capillary rise

$\mathcal{E}$ = Liquid volume fraction

$\mathcal{E}_c$ = Critical liquid fraction after

ρ_{avg} = Average Density

ρ_{liq} = Liquid density

ρ_{gas} = Gas density

V_{liq} = Liquid volume in column

V_{total} = Total foam volume in column

References

Ahmed, R. M., Takach, N. E., Khan, U. M., Taoutaou, S., James, S., Saasen, A., & Godøy, R. (2009). Rheology of foamed cement. Cement and Concrete Research, 39(4), 353–361. https://doi.org/10.1016/J.CEMCONRES.2008.12.004

Ahmed, R., Kuru, E., & Saasen, A. 2003. Critical Review of Drilling Foam Rheology. Annual Transactions of the Nordic Rheology Society, Vol. 11, 63-72.

Akhtar, T.F. 2017. Rheology of Aqueous and Polymer-Based Nitrogen Foams at High Pressure and High Temperature (HPHT) Conditions. Master's Thesis, University of Oklahoma: Norman, Oklahoma.

Akhtar, T.F., Ahmed, R., Elgaddafi, R., Shah, S., Amani, M. 2018. Rheological behavior of aqueous foams at high pressure. J. Pet. Sci. Eng. 162: 214-224.

Argillier, J.-F., Saintpere, S., Herzhaft, B.et al.. 1998. Stability and Flowing Properties of Aqueous Foams for Underbalanced Drilling. Paper presented at the SPE Annual Technical Conference and Exhibition, New Orleans, Louisiana, USA, 27–30 September. SPE-48982-MS. https://doi.org/10.2118/48982-MS.

Barnes, G.T. The effects of monolayers on the evaporation of liquids, Advances in Colloid and Interface Science, Volume 25, 1986, Pages 89-200, ISSN 0001-8686, DOI: https://doi.org/10.1016/0001-8686(86)80004-5.

Benge, O.G., Spangle, L.B., and C.W. Sauer. Foamed Cement - Solving Old Problems with a New Technique. Paper presented at the SPE Annual Technical Conference and Exhibition, New Orleans, Louisiana, September 1982. DOI: https://doi.org/10.2118/11204-MS

Blauer, R.E., and C.A. Kohlhaas. Formation Fracturing with Foam. Paper presented at the Fall Meeting of the Society of Petroleum Engineers of AIME, Houston, Texas, October 1974. DOI: https://doi.org/10.2118/5003-MS

Capo, J., Yu, M., Miska, S.Z., Takach, N., and Ahmed, R. Cuttings Transport with Aqueous Foam at Intermediate-Inclined Wells. *SPE Drill & Compl* 21 (2006): 99–107. DOI: https://doi.org/10.2118/89534-PA

Carrier, V. & Colin, A. (2003). Coalescence in Draining Foams. Langmuir. 19. Doi:10.1021/la026995b.

Cohen, A., Fraysse, N., and Raufaste, C. Drop coalescence and liquid flow in a single Plateau border. Physical Review E: Statistical, Nonlinear, and Soft Matter Physics, American Physical Society, 2015, 91, Doi: http://journals.aps.org/pre/abstract/10.1103/PhysRevE.91.053008

Cox, S.J., Graner, F. Three-dimensional bubble clusters: shape, packing, and growth rate, Phys Rev E, 69 (3) (2004), p. 031409

DOI: https://doi-org.ezproxy.lib.ou.edu/10.2118/206404-MS

Drennan, W., Hutzler, S. Structure and energy of liquid foams, Advances in Colloid and Interface Science, Volume 224, 2015, Pages 1-16, ISSN 0001-8686, https://doi.org/10.1016/j.cis.2015.05.004.

Durand, M. & Langevin, D. (2002). Physicochemical Approach to the Theory of Foam Drainage. European Physical Journal E. 7. 35-44. Doi:10.1140/epje/i200101092.

Eftekhari, A. A., Krastev, R., and Farajzadeh, R. "Foam Stabilized by Fly-Ash Nanoparticles for Enhancing Oil Recovery." Paper presented at the SPE Kuwait Oil and Gas Show and

Conference, Mishref, Kuwait, October 2015. DOI: https://doi-org.ezproxy.lib.ou.edu/10.2118/175382-MS

Falk, K. and McDonald, C. An Overview of Underbalanced Drilling Applications in Canada. Paper presented at the SPE European Formation Damage Conference, The Hague, Netherlands, May 1995. DOI: https://doi.org/10.2118/30129-MS

Fried, A.N. Foam-Drive Process for Increasing the Recovery of Oil, report, 1961; [Washington D.C.]. (https://digital.library.unt.edu/ark:/67531/metadc38691/m1/22/:)

Fuseni, A., Han, M., and Al-Aseeri, A. Evaluation of Foaming Agents for EOR Applications in Carbonate Reservoirs. Paper presented at the SPE EOR Conference at Oil and Gas West Asia, Muscat, Oman, March 2014. DOI: https://doi.org/10.2118/169723-MS

Gajbhiye, R. "Novel CO_2/N_2 Foam Concept and Optimization Scheme for Improving CO_2-foam EOR Process." Paper presented at the SPE Middle East Oil & Gas Show and Conference, event canceled, November 2021. DOI: https://doi.org/10.2118/204852-MS

Govindu, A. 2019. Drainage Behavior of Aqueous, Polymeric, and Oil-Based Nitrogen Foams: Theoretical and Experimental Investigation. Ph.D. Thesis, University of Oklahoma, Norman, Oklahoma

Govindu, A., Ahmed, R., Shah, S., and Amani, M. Foam Stability - Does Well Inclination Matter? Paper presented at the SPE/ICoTA Well Intervention Conference and Exhibition, The Woodlands, Texas, USA, March 2020. DOI: https://doi-org.ezproxy.lib.ou.edu/10.2118/199821-MS

Govindu, A., Ahmed, R., Shah, S., and Amani, M. The Effect of Inclination on the Stability of Foam Systems in Drilling and Well Operations. *SPE Drill & Compl* 36 (2021): 263–280. DOI: https://doi.org/10.2118/199821-PA

Gu, M. and Mohanty, K. Rheology of polymer-free foam fracturing fluids, Journal of Petroleum Science and Engineering, Volume 134, 2015, Pages 87-96, ISSN 0920-4105, https://doi.org/10.1016/j.petrol.2015.07.018.

Harkins, W.D. J. Chem. Phys. 9, 552 (1941); Submitted: 21 March 1941 • Published Online: 29 December 2004, DOI: https://doi.org/10.1063/1.1750953

Harris, P.C. 1989. Effects of Texture on Rheology of Foam Fracturing Fluids. SPE Production Engineering 4 (03): 249–257.

Hilgenfeldt, S., Koehler, S. A., and Stone, H. A. Dynamics of Coarsening Foams: Accelerated and Self-Limiting Drainage, 2001, Doi: https://link.aps.org/doi/10.1103/PhysRevLett.86.4704

Hill, C., & Eastoe, J. (2017). Foams: From nature to industry. Advances in Colloid and Interface Science, 247, 496-513. https://doi.org/10.1016/j.cis.2017.05.013

Holt, T., Vassenden, F., and Svorstol, I. Effects of Pressure on Foam Stability; Implications for Foam Screening. Paper presented at the SPE/DOE Improved Oil Recovery Symposium, Tulsa, Oklahoma, April 1996. DOI: https://doi.org/10.2118/35398-MS

Kraynik, A M. Foam drainage. (1983) United States. https://doi.org/10.2172/5518540

Kim, A.K. and Dlugogorski, B.Z.1997. Multipurpose Overhead Compressed-Air Foam System and Its Fire Suppression Performance. J. Fire Protection Eng.8 (3): 133–150. https://doi.org/10.1177/104239159600800303

Koczo, K. Lobo, L.A., Wasan, D. T. Effect of oil on foam stability: Aqueous foams stabilized by emulsions, Journal of Colloid and Interface Science, Volume 150, Issue 2, 1992, Pages 492-506, ISSN 0021-9797, DOI: https://doi.org/10.1016/0021-9797(92)90218-B.

Koehler, S., Stone, H.A., Brenner, M. and Eggers, J. (1998). Dynamics of Foam Drainage. Phys. Rev. E. 58. 10.1103/PhysRevE.58.2097.

Koehler, S. A., Hilgenfeldt, S., & Stone, H. A. (2000). A generalized view of foam drainage: experiment and theory. *Langmuir*, *16*(15), 6327-6341.

Kovscek, A. R. and Radke, C. J. Foams: Fundamentals and Applications in the Petroleum Industry. October 15, 1994, 115-163. DOI: https://doi.org/10.1021/ba-1994-0242.ch003

Kristiansen, T.S., and Holt, T. "Properties of Flowing Foam in Porous Media Containing Oil." Paper presented at the SPE/DOE Enhanced Oil Recovery Symposium, Tulsa, Oklahoma, April 1992. DOI: https://doi-org.ezproxy.lib.ou.edu/10.2118/24182-MS

Kruglyakov, P. M., Karakashev, S. I., Nguyen, A. V.et al.. 2008. Foam Drainage. Curr Opin Colloid Interface Sci13 (3): 163–170. https://doi.org/10.1016/j.cocis.2007.11.003.

Kumar, A., Dutt, A, Singh, S., Sikarwar, S.S., Das, R., and Kishore, K. Prospects of Foam Stimulation in Oil and Gas Wells of India. Paper presented at the Trinidad and Tobago Energy Resources Conference, Port of Spain, Trinidad, June 2010. DOI: https://doi.org/10.2118/132268-MS

Li, Z., Liu, Z. , Li, B. , Li, S. , Sun, Q. , and Wang, S. "Aqueous Foams Stabilized with Particles and Surfactants." Paper presented at the SPE Saudi Arabia Section Technical Symposium and Exhibition, Al-Khobar, Saudi Arabia, April 2012. DOI: https://doi-org.ezproxy.lib.ou.edu/10.2118/160840-MS

Lourenco, A., Miska, S., Reed, T., Pickell, M., and Takach, N. Study of the Effects of Pressure and Temperature on the Viscosity of Drilling Foams and Frictional Pressure Losses. Paper presented at the SPE Annual Technical Conference and Exhibition, Denver, Colorado, October 2003. DOI: https://doi.org/10.2118/84175-MS

Martins, A. L., Lourenço, A. M. F., and C. H. M. de Sá. Foam Property Requirements for Proper Hole Cleaning While Drilling Horizontal Wells in Underbalanced Conditions. *SPE Drill & Compl* 16 (2001): 195–200. DOI: https://doi.org/10.2118/74333-PA

Mensire, R. & Lorenceau, E. (2017). Stable oil-laden foams: Formation and evolution. Advances in Colloid and Interface Science. 247. Doi: 10.1016/j.cis.2017.07.027.

Mitchell, B.1971. Test Data Fill Theory Gap on using Foam as a Drilling Fluid. Oil and Gas Journal, 96-100.

Obisesan O, Ahmed R, Amani M. The Effect of Salt on Stability of Aqueous Foams. *Energies*. 2021; 14(2):279. https://doi.org/10.3390/en14020279

Obisesan, O. Stability of Aqueous Foams at High Pressure and the Impact of Contaminants / by Oyindamola Obisesan. (2021). Web.

Omar, B.A., Al Moajil, A.A., Al-Darweesh, S., and Al-Rustum, A. Evaluation of Novel Surfactant for Acid Stimulation and EOR Treatments. Paper presented at the IADC/SPE Asia Pacific Drilling Technology Conference and Exhibition, Bangkok, Thailand, August 2018. DOI: https://doi.org/10.2118/191115-MS

Ortiz, D., Izadi, M., and Kam, S. I. "Modeling of Nanoparticle-Stabilized CO_2 Foam Enhanced Oil Recovery." *SPE Res Eval & Eng* 22 (2019): 971–989. DOI: https://doi.org/10.2118/194018-PA

Ozbayoglu, M. E., Akin, S., and Eren, T. "Analysis of the Influence of Bubble Size and Texture on Foam Characterization." Paper presented at the 12th International Conference on Multiphase Production Technology, Barcelona, Spain, May 2005. Doi: https://doi-org.ezproxy.lib.ou.edu/10.2118/162712-PA

Parvaneh, R., Riahi, S., and Lotfollahi, M. N. "Experimental Evaluation of a Polymer Foam Agent on the Foam Stability, Concern to Surfactant, Nanoparticle, and Salinity." *SPE J.* (2022;): DOI: https://doi-org.ezproxy.lib.ou.edu/10.2118/209209-PA

Peskunowicz, J.J., and D.L. Bour. Foam Cement Solves Cementing Problems in Alberta, Canada. Paper presented at the Annual Technical Meeting, Calgary, Alberta, June 1987. DOI: https://doi.org/10.2118/87-38-89

Plateau, J. Experimental and Theoretical Statics of Liquids Subject to Molecular Forces Only,1873

Qian, C., Telmadarreie, A., Dong, M., and Bryant, S. "Synergistic Effect between Surfactant and Nanoparticles on the Stability of Foam in EOR Processes." *SPE J.* 25 (2020): 883–894. Doi: https://doi-org.ezproxy.lib.ou.edu/10.2118/195310-PA

Rand, P., and Kraynik, A. Drainage of Aqueous Foams: Generation-Pressure and Cell-Size Effects." *SPE J.* 23 (1983): 152–154. DOI: https://doi.org/10.2118/10533-PA

Rio, E., Drenckhan, W., Salonen, A., Langevin, D. Unusually stable liquid foams, Advances in Colloid and Interface Science, Volume 205, 2014, Pages 74-86, ISSN 0001-8686, https://doi.org/10.1016/j.cis.2013.10.023.

Robinson, J. V., & Woods, W. W. (1948). A method of selecting foam inhibitors. *Journal of the Society of Chemical Industry*, *67*(9), 361-365.

Ruckenstein, E., Jain, R.K. 1974. Spontaneous Rupture of Thin Liquid Films. Journal of Colloid Science, (1974) 70, 132 – 147.

Saint-Jalmes, A., Vera, M. U., & Durian, D. J. (2000). Free Drainage of Aqueous Foams: Container Shape Effects on Capillarity and Vertical Gradients. Europhysics Letters, 50 (5), 695-701. http://dx.doi.org/ 10.1209/epl/i2000-00326-y

Saint-Jalmes, A., Zhang, Y., & Langevin, D. (2004). Quantitative description of foam drainage: Transitions with surface mobility. *The European Physical Journal E, 15*(1), 53-60.

Saint-Jalmes, Arnaud. (2006). Physical chemistry in foam drainage and coarsening. Soft Matter. 2. Doi:10.1039/b606780h.

Schramm, L.L., and Novosad, J.J., 1990. Micro-visualization of foam interactions with crude oil. Colloids Surfaces, 46: 21-43.

Schramm, L.L., Novosad, J.J. The destabilization of foams for improved oil recovery by crude oils: Effect of the nature of the oil, Journal of Petroleum Science and Engineering, Volume 7, Issues 1–2, 1992, Pages 77-90, ISSN 0920-4105, Doi: https://doi.org/10.1016/0920-4105(92)90010-X.

Shehzad, A., Waleed, A., Waqas, A. and Khan, S. Deep Learning Approach to Predict Rheological Behavior of $scCO_2$ Foam Fracturing Fluid Under Different Operating Conditions. Paper presented at the Abu Dhabi International Petroleum Exhibition & Conference, Abu Dhabi, UAE, November 2020. DOI: https://doi-org.ezproxy.lib.ou.edu/10.2118/202679-MS

Sheng, J. J. (Ed.). (2013). *Enhanced oil recovery field case studies*. Gulf Professional Publishing.

Sherif, T., Ahmed, R., Shah, S., Amani, M. 2016. Rheological correlations for oil-based drilling foams. Journal of Natural Gas Science and Engineering, 35, 1249–1260.

Simjoo, M., Dong, Y., Andrianov, A., Telangana, M., and P.L.J. L.J. Zitha. Novel Insight into Foam Mobility Control. *SPE J.* 18 (2013): 416–427. DOI: https://doi.org/10.2118/163092-PA

Singh, R., and Mohanty, K. Nanoparticle-Stabilized Foams for High-Temperature, High-Salinity Oil Reservoirs. Paper presented at the SPE Annual Technical Conference and Exhibition, San Antonio, Texas, USA, October 2017. DOI: https://doi.org/10.2118/187165-MS

Tcholakova, S., Denkov, N. D., & Lips, A. (2008). Comparison of solid particles, globular proteins, and surfactants as emulsifiers. *Physical Chemistry Chemical Physics*, *10*(12), 1608-1627.

Telmadarreie, A. and Trivedi, J. (2018). Static and Dynamic Performance of Wet Foam and Polymer-Enhanced Foam in the Presence of Heavy Oil. Colloids and Interfaces. 2. 38. Doi:10.3390/colloids2030038.

Thomas, G.L., Belmonte, J.M., Graner, F., Glazier, J.A., de Almeida, R.M. 3D simulations of wet foam coarsening evidence a self-similar growth regime. Colloids and surfaces. A, Physicochemical and Engineering Aspects. 2015 May; 473:109-114. DOI: 10.1016/j.colsurfa.2015.02.015. PMID: 27630449; PMCID: PMC5019577.

Vikingstad, A.K., Skauge, A., Høiland, H., Aarra, M. Foam–oil interactions analyzed by static foam tests, Colloids and Surfaces A: Physicochemical and Engineering Aspects, Volume 260, Issues 1–3, 2005, Pages 189-198, ISSN 0927-7757, https://doi.org/10.1016/j.colsurfa.2005.02.034.

Wasan, D.T., Koczo, K., Nikolov, A.D., Schramm, L.L. Foams: Fundamentals and Application in the Petroleum Industry, The American Chemical Society, Washington, DC (1994)

Weaire, D., & Pageron, V. (1990). Frustrated froth: Evolution of foam inhibited by an insoluble gaseous component. Philosophical magazine letters, 62(6), 417-421.

Wei, B., Chen, S., Tian, Q., and Lu, J. "Conformance Control in Fractured Tight Formations using Functional Nanocellulosic Materials Reinforced CO2 Foam Systems." Paper

presented at the SPE Annual Technical Conference and Exhibition, Virtual, October 2020. doi: https://doi-org.ezproxy.lib.ou.edu/10.2118/201671-MS

Worthen, A., Bagaria, H., Chen, Y, Bryant, S., Huh, C, and Johnston, K. Nanoparticle Stabilized Carbon Dioxide in Water Foams for Enhanced Oil Recovery. Paper presented at the SPE Improved Oil Recovery Symposium, Tulsa, Oklahoma, USA, April 2012. DOI: https://doi.org/10.2118/154285-MS

Zhou, J., Ranjith, P.G., Wanniarachchi, W.A.M. Different strategies of foam stabilization in the use of foam as a fracturing fluid. Advances in Colloid and Interface Science, Volume 276, 2020, 102104, ISSN 0001-8686, https://doi.org/10.1016/j.cis.2020.102104.

Zhu, Y., Tian, J., Hou, Q., Luo, Y., and Fan, J. Studies on Nanoparticle-Stabilized Foam Flooding EOR for a High Temperature and High Salinity Reservoir. Paper presented at the Abu Dhabi International Petroleum Exhibition & Conference, Abu Dhabi, UAE, November 2017. DOI: https://doi.org/10.2118/188964-MS

Zvada, M.V., Belovus, P. N., Sergeev, E. I., Glavnov, N. G., Varfolomeev, M. A., and Saifullin, E. R. "Study of the Efficiency of Gel and Polymer-Stabilized Foam Systems for Gas Shut-Off in Horizontal Wells." Paper presented at the SPE Russian Petroleum Technology Conference, Virtual, October 2021.

Appendix A: Foam Quality Profile

A.1 Effect of pressure with 10% oil contamination

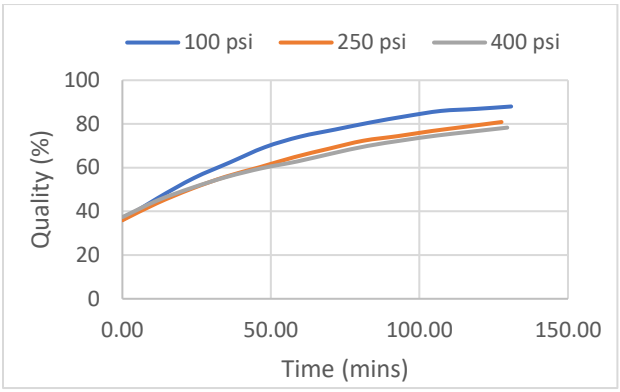

(a)

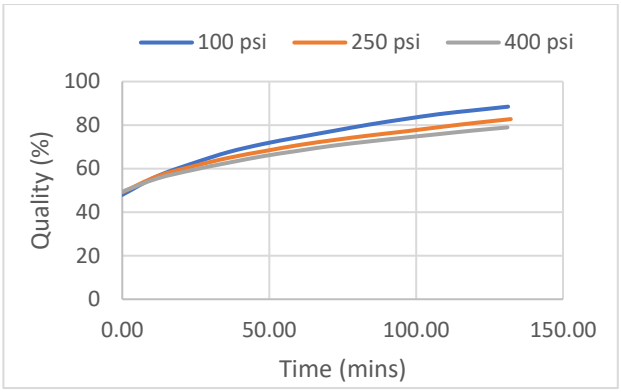

(b)

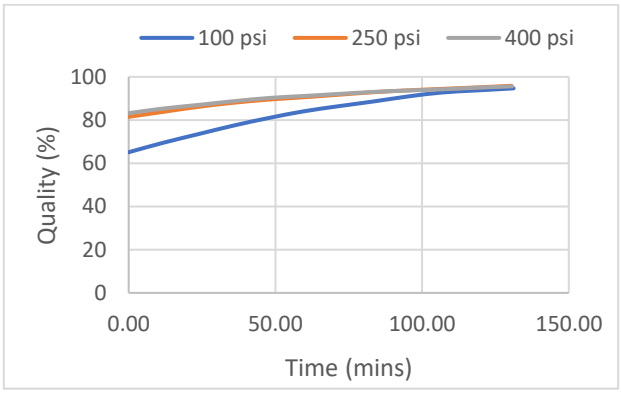

(c)

Appendix A 1: Foam quality profile for the drainage test for aqueous foams of different foam qualities with 10 % oil contamination (a) 40%, (b) 50%, and (c) 60%

A.2 Effect of pressure with 20% oil concentration

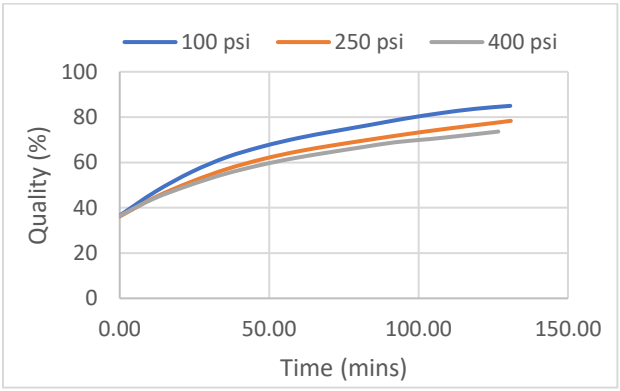

(a)

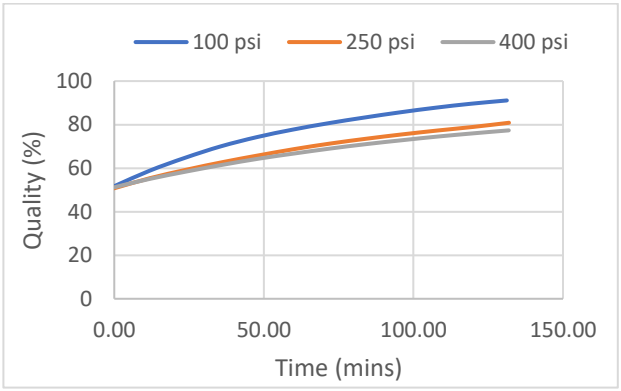

(b)

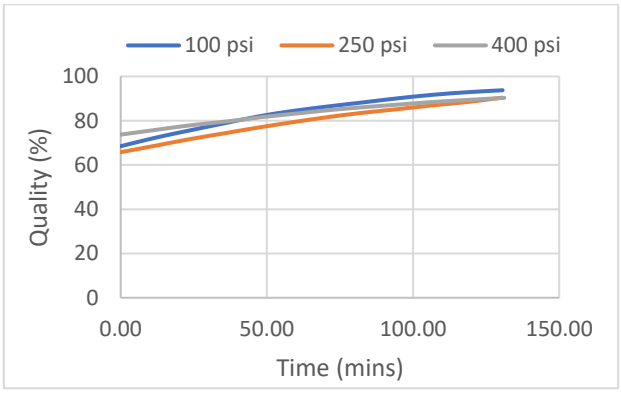

(c)

Appendix A 2: Foam quality profile for the drainage test for aqueous foams of different foam qualities with 20 % oil contamination (a) 40%, (b) 50%, and (c) 60%

Appendix B: Foam Density Profile

B.1 Effect of pressure with 10% oil contamination

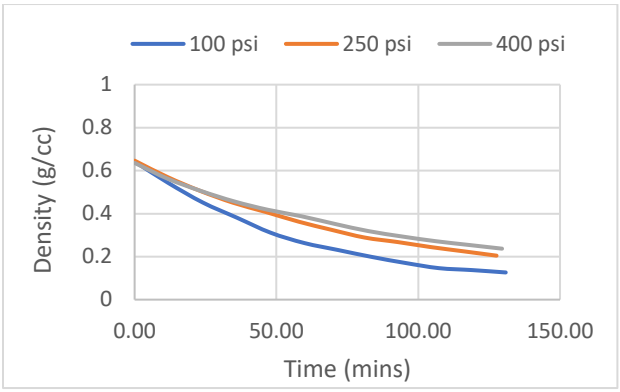

(a)

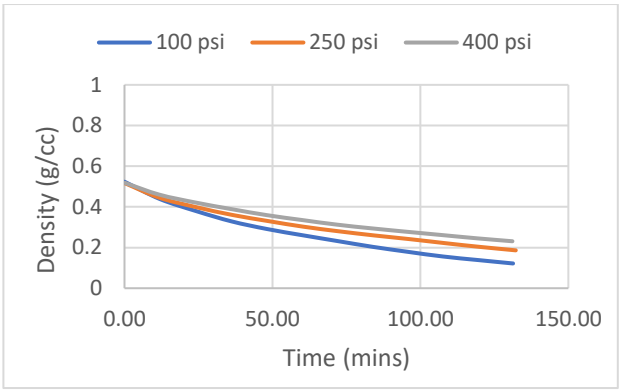

(b)

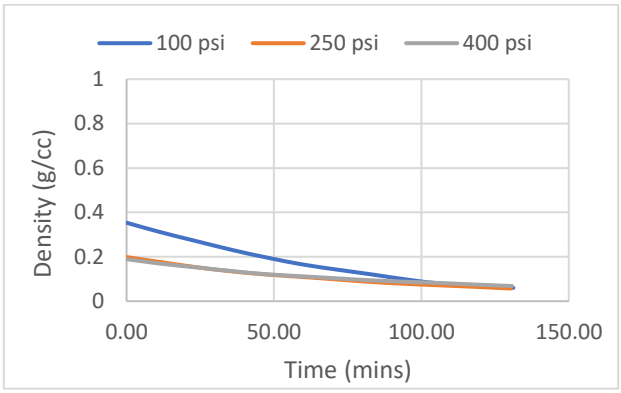

(c)

Appendix B 1: Foam density profile for the drainage test for aqueous foams of different foam qualities with 10% oil contamination (a) 40%, (b) 50%, and (c) 60%

B.2 Effect of pressure with 20% oil contamination

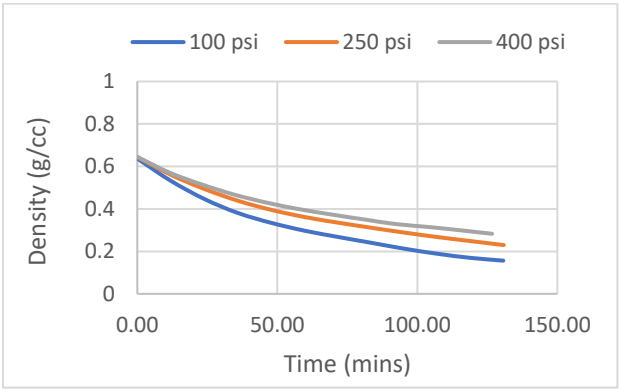

(a)

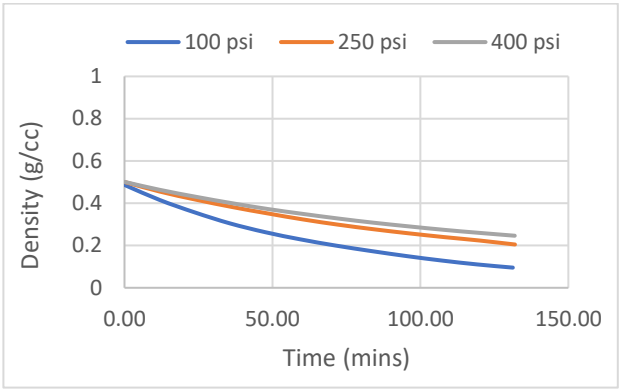

(b)

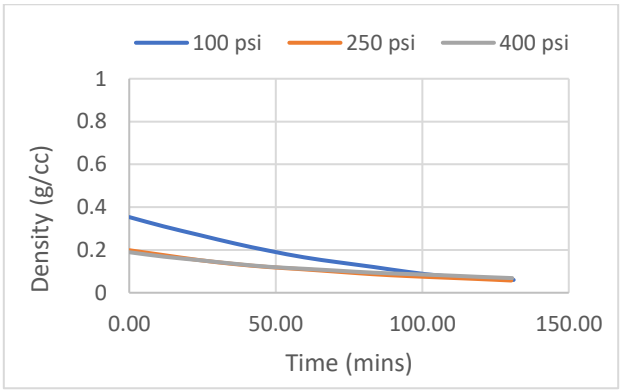

(c)

Appendix B 2: Foam density profile for the drainage test for aqueous foams of different foam qualities with 20% oil contamination (a) 40%, (b) 50%, and (c) 60%